REGISTERED No. M. 3121

PROCEEDINGS

OF THE

INDIAN ACADEMY

OF SCIENCES

VOL. XXXIX] *SECTION A* [No. 2

FEBRUARY 1954

UNIVERSITY
OF MICHIGAN
APR 2
ENGINEERING
LIBRARY

Price Rs. 2 or 3 Sh. *Annual Subscription Rs. 18*

PRINTED AT THE BANGALORE PRESS, BANGALORE CITY, BY C. VASUDEVA RAO,
SUPERINTENDENT AND PUBLISHED BY THE INDIAN ACADEMY OF
SCIENCES, BANGALORE.

X-RAY ANTI-REFLECTIONS IN CRYSTALS

Part II. Calculation of the Integrated Reflection and Integrated Anti-Reflection for an Internal Reflection

By G. N. Ramachandran, F.A.Sc.

(Department of Physics, University of Madras, Guindy, Madras-25)

Received December 21, 1953

1. Introduction

The influence of the state of perfection of a crystal on the integrated reflection was considered by Hirsch and the author (1950) for the case of a surface reflection. The present paper deals with a similar study for an internal reflection, *i.e.*, when both the incident and reflected beams pass through the thickness of the crystal. The basic theory for an internal reflection is contained in the dynamical theory of Ewald (1916), which has been amplified and put in a more tractable form recently by Zachariasen (1945) and Laue (1949). Using these, the interesting observations of Campbell (1951) on the occurrence of sharp maxima in the transmitted beam have been explained by the author (1952 *a*, *b*) and independently by Hirsch (1952). This phenomenon has been termed " anti-reflection " by the author, and arises essentially from a decrease in the absorption coefficient near a reflection maximum, as has been pointed out by Laue (1949) and shown to be quantitatively true by Zachariasen (1952).

In the present paper we shall consider the variations of the reflected and transmitted intensities with various factors such as absorption coefficient, structure factor, asymmetry and thickness of the crystal. It is found that Laue's equations, which formed the basis of the previous paper of the author (Ramachandran and Kartha, 1952 *b*, hereafter referred to as Part I), are not accurate enough as they had been obtained by putting in certain approximations in the very beginning. Consequently, more complete expressions are worked out here and the approximations for special cases are obtained later.

The notation of Part I will be used in this paper, and reference may be made to Section 3 of that paper for the explanation of the symbols. Additional symbols used are collected together in the next section for ready reference.

2. NOTATION

$\mathrm{P} = \frac{\mu \mathrm{D}}{2}\left(\frac{1}{\gamma_0} + \frac{1}{\gamma_h}\right)$, product of the absorption coefficient and the mean path through the crystal of the reflected and transmitted beams.

$\mathrm{G} = g/a$, parameter depending on the relative values of absorption coefficient and structure factor.

$a = (1-b)/(1+b)$, asymmetry factor.

$\mathrm{X} = [(y^2 - a^2\mathrm{G}^2 + 1 - k^2) + i(k + ay\mathrm{G})]^{\frac{1}{2}}$

$j = (a^2 + k^2/\mathrm{G}^2)^{\frac{1}{2}}$

$\phi = \tan^{-1} a\mathrm{G}/k.$

$\mathrm{R}_y = \int_{-\infty}^{+\infty} \mathrm{R}\,dy$, integrated reflection in y-units.

$\mathrm{T}_y = \int_{-\infty}^{+\infty} (\mathrm{T} - e^{-\mu \mathrm{D}/\gamma_0})\,dy$, integrated transmission in y-units.

3. EXACT EXPRESSIONS FOR R AND T IN THE CASE OF AN INTERNAL REFLECTION

We have the following equations from Laue's paper:

$$\mathrm{D}_{01} = \frac{e^{-\nu}}{2\cosh \nu}\,\mathrm{D}_0^{(a)} \quad ; \quad \mathrm{D}_{02} = \frac{e^{+\nu}}{2\cosh \nu}\,\mathrm{D}_0^{(a)} \tag{1}$$

$$\mathrm{D}_{h1} = \frac{-\sqrt{b}}{2\cosh \nu}\left[\frac{\chi_{\bar{h}}}{\chi_h}\right]^{\frac{1}{2}} \mathrm{D}_0^{(a)} \; ; \quad \mathrm{D}_{h2} = \frac{+\sqrt{b}}{2\cosh \nu}\left[\frac{\chi_{\bar{h}}}{\chi_h}\right]^{\frac{1}{2}} \mathrm{D}_0^{(a)}, \tag{2}$$

where $\sinh \nu = \beta_h \sqrt{b}/2\mathrm{C}\,[\chi_h \chi_{\bar{h}}]^{\frac{1}{2}}$ (3)

Introducing the variable

$$\epsilon_h = b\beta_h/2 = b\alpha_h + \chi_0(1-b)/2, \tag{4}$$

we have

$$\sinh \nu = \epsilon_h/\mathrm{C}\sqrt{b}\,[\chi_h\,\chi_{\bar{h}}]^{\frac{1}{2}} \tag{5}$$

The boundary conditions give the equations*

$$\mathrm{D}_{01} \exp[-2\pi i (\mathbf{R}_{01}\cdot\mathbf{z})\,\mathrm{D}] + \mathrm{D}_{02} \exp[-2\pi i (\mathbf{R}_{02}\cdot\mathbf{z})\,\mathrm{D}] = \mathrm{D}_0^{(d)} \exp[-2\pi i (\mathbf{R}_0^{(d)}\cdot\mathbf{z})\,\mathrm{D}] \tag{6a}$$

$$\mathrm{D}_{h1} \exp[-2\pi i (\mathbf{R}_{h1}\cdot\mathbf{z})\,\mathrm{D}] + \mathrm{D}_{h2} \exp[-2\pi i (\mathbf{R}_{h2}\cdot\mathbf{z})\,\mathrm{D}] = \mathrm{D}_h^{(d)} \exp[-2\pi i (\mathbf{R}_h^{(d)}\cdot\mathbf{z})\,\mathrm{D}] \tag{6b}$$

* The corresponding Eq. (6) in Part I contains a small obvious error, which, however, does not affect the final results.

Here

$$\mathbf{R}_{h1,2} = \mathbf{R}_{01,2} + \mathbf{b}_h$$

and

$$\mathbf{R}_{01,2} = \mathbf{R}_0^{(a)} - k\delta_{1,2}\mathbf{z} \tag{7}$$

where

$$\delta_{1,2} = \frac{1}{2\gamma_0}(\epsilon_h - \chi_0) \pm \frac{1}{2\gamma_0}(\epsilon_h^2 + bC^2\chi_h\chi_{\bar{h}})^{\frac{1}{2}}, \tag{8}$$

the positive sign referring to field No. 1 and the negative sign to field No. 2. Thus,

$$|D_h^{(d)}|^2 = |D_{h1}\exp(2\pi ik\delta_1 D) - D_{h2}\exp(2\pi ik\delta_2 D)|^2.$$

Writing

$$\sigma_{1,2} = 4\pi k \operatorname{Im}(\delta_{1,2}) \text{ and } \Delta_{1,2} = -4\pi k \operatorname{Re}(\delta_{1,2}), \tag{9}$$

where the symbols Im and Re stand for the imaginary and real parts of δ, we have

$$R = \frac{1}{b}\left|\frac{D_h^{(d)}}{D_0^{(d)}}\right|^2 = \frac{\exp[-\frac{1}{2}(\sigma_1+\sigma_2)D]}{2|\cosh v|^2}\left|\frac{\chi_{\bar{h}}}{\chi_h}\right| \times[\cosh\tfrac{1}{2}(\sigma_1-\sigma_2)D - \cos\tfrac{1}{2}(\Delta_1-\Delta_2)D] \tag{10}$$

From Eqn. (6 *a*), the corresponding expression for the transmission T can readily be shown to be

$$T = \left|\frac{D_0^{(d)}}{D_0^{(d)}}\right|^2 = \frac{\exp[-\frac{1}{2}(\sigma_1+\sigma_2)D]}{2|\cosh v|^2}[\cosh\{\tfrac{1}{2}(\sigma_1-\sigma_2)D + 2v_r\} + \cos\{\tfrac{1}{2}(\Delta_1-\Delta_2)D + 2v_i\}] \tag{11}$$

Equations (10) and (11) do not use the approximation adopted by Laue, namely, that the imaginary part of v is small, and that $|\cosh v|^2 = \cosh^2 v_r$.

4. Formulae for Centro-Symmetric Crystals

When a crystal possesses a centre of symmetry, the symmetry operation of inversion requires that $\chi_h = \chi_{\bar{h}}$.

Under these conditions,

$$\chi_h\chi_{\bar{h}} = \chi_h^2 \text{ and } |\chi_h/\chi_{\bar{h}}| = 1.$$

Thus,

$$\sinh v = \epsilon_h/C\sqrt{b}\chi_h \tag{12}$$

and

$$\delta_{1,2} = \frac{1}{2\gamma_0}(\epsilon_h - \chi_0) \pm \frac{1}{2\gamma_0}(\epsilon_h^2 + bC^2\chi_h^2)^{\frac{1}{2}}. \tag{13}$$

Defining

$$\left.\begin{aligned} y &= \epsilon_{hr}/C \mid \chi_{hr} \mid b^{\frac{1}{2}} \\ g &= \epsilon_{hi}/C \mid \chi_{hr} \mid b^{\frac{1}{2}} \\ k &= \chi_{hi}/\chi_{hr} \end{aligned}\right\} \tag{14}$$

we have

$$\sinh v = (y + ig)/(1 + ik) \tag{15}$$

One thus obtains the following expressions for the various quantities occurring in Eqs. (10) and (11) in terms of the parameters y, g, k, which are the same as those used by Zachariasen (1945).

$$\cosh^2 v = [(y + ig)^2 + (1 - k^2 + 2ik)]/(1 - k^2 + 2ik)$$

$$|\cosh^2 v| = [(y^2 - g^2 + 1 - k^2)^2 + 4(k + yg)^2]^{\frac{1}{2}}/(1 + k^2) \tag{16}$$

$$\tfrac{1}{2}(\sigma_1 + \sigma_2) = -2\pi k \chi_{0i}(1 + b)/2\gamma_0 = \mu(1 + b)/2\gamma_0$$

$$\tfrac{1}{2}(\sigma_1 - \sigma_2) = [2\pi k C \chi_{hr}/\sqrt{\gamma_h \gamma_0}] \operatorname{Im}[(y^2 - g^2 + 1 - k^2) + 2i(k + yg)]^{\frac{1}{2}}$$

$$\tfrac{1}{2}(\Delta_1 - \Delta_2) = [2\pi k C \chi_{hr}/\sqrt{\gamma_h \gamma_0}] \operatorname{Re}[(y^2 - g^2 + 1 - k^2) + 2i(k + yg)]^{\frac{1}{2}}$$

Defining a new parameter

$$G = \tfrac{1}{2}\chi_{0i}(1 + b)/C\sqrt{b} \mid \chi_{hr} \mid = g/a, \tag{17}$$

where a is the asymmetry factor

$$a = (1 - b)/(1 + b) \tag{18}$$

we have

$$2\pi k C \chi_{hr}/\sqrt{b} = \frac{2\pi k \chi_{0i}}{G} \frac{(1 + b)}{2\gamma_0} = -\frac{\mu}{G} \frac{(1 + b)}{2\gamma_0} .$$

Writing

$$\mu D(1 + b)/2\gamma_0 = \frac{\mu D}{2}\left(\frac{1}{\gamma_0} + \frac{1}{\gamma_h}\right) = P, \tag{19}$$

which is only an obvious generalisation of the definition of P in Part I, we have

$$R = \frac{e^{-P}(1 + k^2)}{2|X|^2}\left[\cosh\left(\frac{P}{G} \operatorname{Im} X\right) - \cos\left(\frac{P}{G} \operatorname{Re} X\right)\right], \tag{20}$$

$$T = \frac{e^{-P}(1 + k^2)}{2|X|^2}\left[\cosh\left(\frac{P}{G} \operatorname{Im} X - 2v_r\right) + \cos\left(\frac{P}{G} \operatorname{Re} X - 2v_i\right)\right], \tag{21}$$

where

$$X = [(y^2 - a^2G^2 + 1 - k^2) + 2i(k + ayG)]^{\frac{1}{2}} \tag{22}$$

On making the approximations $k \ll 1$ and $v_i \ll 1$, one obtains Eqns. (8) and (9) of Part I, which were deduced directly from Laue's paper.

5. Expressions for Integrated Reflection

All the quantities occurring in Eqns. (20) and (21) are constant parameters for a particular reflection of a crystal, except y, which is proportional to the angular deviation from the exact Bragg setting. Thus, a graph of R (or T) against y represents the Bragg reflection (or anti-reflection) curve. Except in special experiments, employing high resolution, one is interested in general, not in the shape or breadth of this curve, but in the " integrated " quantity, which is the area enclosed between this curve and the axis of abscissæ. The integrated reflection (or anti-reflection) in y-units, *viz.*, $\int_{-\infty}^{+\infty} \mathrm{R}\,dy$ is actually proportional to the integrated reflection, as usually understood, *viz.*, $\int_{-\infty}^{+\infty} \mathrm{R}\,d(\theta - \theta_B)$, the relation between the two being given by

$$\int \mathrm{R}\,d(\theta - \theta_B) = \frac{\mathrm{C}\,|\,\chi_h\,|}{\sqrt{b}\,\sin 2\theta_B} \int \mathrm{R}\,dy \tag{23}$$

Consequently, we shall only use the former to represent the integrated reflection, and denote it by the symbol R_y (or T_y as the case may be).

The integration may be carried out analytically in a few cases and we shall consider these below:

(*a*) For a symmetrical reflection, $a = 0$, and if k is small, so that $k^2 \ll 1$, then we have

$$\mathrm{X} \simeq [(y^2 + 1) + 2ik]^{\frac{1}{2}} = (y^2 + 1)^{\frac{1}{2}} + ik/(y^2 + 1)^{\frac{1}{2}}$$

and

$$|\,\mathrm{X}\,|^2 = (y^2 + 1)$$

Thus,

$$\mathrm{R}_y = \frac{e^{-\mathrm{P}}}{2} \int_{-\infty}^{+\infty} \frac{1}{(y^2 + 1)} \left[\cosh \frac{\mathrm{P}k}{\mathrm{G}\sqrt{y^2 + 1}} - \cos \frac{\mathrm{P}\sqrt{y^2 + 1}}{\mathrm{G}} \right] dy$$

which may be put in the form:

$$\mathrm{R}_y = \frac{e^{-\mathrm{P}}}{2} \left[\int_{-\pi/2}^{\pi/2} \cosh \left(\frac{\mathrm{P}k \cos \theta}{\mathrm{G}} \right) d\theta - \int_{-\infty}^{+\infty} \frac{\cos\,[\mathrm{P}\,(\cosh t)/\mathrm{G}]}{\cosh\, t}\, dt \right].$$

Both the integrals can be expressed in terms of standard Bessel Functions, so that we have

$$R_y = \frac{\pi}{2} e^{-P}\left[I_0(kP/G) - 1 + \int_0^{P/G} J_0(x)\,dx\right] \tag{24}$$

$$= \frac{\pi}{2} e^{-P}\left[I_0(kP/G) - 1 + 2\sum_{n=0}^{\infty} J_{2n+1}(P/G)\right] \tag{25}$$

(*b*) Another special case in which the expression (20) can be integrated in analytical terms is when $a \neq 0$, but aG is small, so that $a^2G^2 \ll 1$, with $k^2 \ll 1$ as previously.

Under these conditions, we have

$$X \simeq [(y^2 + 1) + 2i(k + aGy)]^{\frac{1}{2}}$$

$$= (y^2 + 1)^{\frac{1}{2}} + i(k + aGy)/(y^2 + 1)^{\frac{1}{2}}$$

and

$$|X|^2 = y^2 + 1, \text{ as before.}$$

The integral R_y can now be put in the form

$$R_y = \frac{e^{-P}}{2}\left[\int_{-\pi/2}^{\pi/2} \cosh\left[jP\cos(\theta - \phi)\right] d\theta - \int_{-\infty}^{+\infty} \frac{\cos\left[(P/G)\cosh t\right]}{\cosh t}\, dt\right]$$

where

$$j^2 = a^2 + (k/G)^2 \text{ and } \tan\phi = aG/k. \tag{26}$$

Thus,

$$R_y = \frac{\pi}{2} e^{-P}\left[I_0(jP) - 1 + \int_0^{P/G} J_0(x)\,dx\right]. \tag{27}$$

Obviously this reduces to Eqn. (24) of case (*a*) when $a = 0$.

(*c*) Another special case in which the expression (20) for R can be integrated is when $a \neq 0$ and $G^2 \gg 1$. Under these conditions, one has

$$X \simeq [y^2 - a^2G^2 + 2iayG]^{\frac{1}{2}} = [y + iaG]$$

and

$$|X|^2 = y^2 + a^2G^2.$$

Thus,

$$R_y = \frac{e^{-P}(1 + k^2)}{2} \int_{-\infty}^{+\infty} [\cosh aP - \cos(Py/G)]/(y^2 + a^2G^2)\,dy.$$

Now,

$$\int_{-\infty}^{+\infty} dy/(y^2 + a^2G^2) = \pi/aG$$

and

$$\int_{-\infty}^{+\infty} \cos(Py/G)\, dy/(y^2 + a^2G^2) = \pi e^{-|aP|}/|aG|$$

(Madelung, 1950), so that

$$R_y = \frac{\pi(1+k^2)}{2|aG|}\, e^{-P}(\cosh aP - e^{-|aP|})$$

$$= \frac{\pi}{2G}(1+k^2)\, e^{-P}\frac{\sinh aP}{a} \tag{28}$$

As will be shown below, this is identical with the corresponding integrated reflection in y-units for a mosaic crystal.

6. Expressions for Integrated Anti-Reflection

The integrated anti-reflection in y-units will be denoted by the symbol T_y and is defined as

$$T_y = \int_{-\infty}^{+\infty} (T - e^{-\mu D/\gamma_0})\, dy. \tag{29}$$

Here, $\exp(-\mu D/\gamma_0)$ is the fraction of the incident intensity which is normally transmitted in the absence of Bragg reflection, and the integrated anti-reflection is the integral over various settings of the excess (or defect) of the actual transmission over this background.

(*a*) *Symmetrical Case.*—Here, $a = 0$, which corresponds to case (*a*) of the previous section and the integration may be carried out analytically. Thus, taking $k^2 \ll 1$ as before, one has

$$T = \frac{e^{-P}}{2(1+y^2)}\left[\cosh\left(\frac{P}{G}\operatorname{Im} X - 2v_r\right) + \cos\left(\frac{P}{G}\operatorname{Re} X - 2v_i\right)\right]. \tag{30}$$

Now,

$$\sinh v = y/(1+ik) = y - iky, \tag{31}$$

so that, within the limits of approximation adopted here,

$$\left.\begin{aligned} &\sinh v_r = y, && \sin v_i = -ky/(y^2+1)^{\frac{1}{2}} \\ &\cosh 2v_r = 1 + 2y^2, && \cos 2v_i = 1 \end{aligned}\right\} \tag{32}$$

Also, in the symmetrical case,

$$e^{-\mu D/\gamma_0} = e^{-P}.$$

On expanding the cosh and cos functions within the square brackets in (30) into products of similar functions, all the odd functions of y drop out of the integral, since the range of integration is from $-\infty$ to $+\infty$, so that we have

$$T_y = e^{-P} \int_{-\infty}^{+\infty} \left[\frac{\cosh 2v_r}{2(1+y^2)} \cosh (Pk/G\sqrt{y^2+1}) + \frac{\cos 2v_i}{2(1+y^2)} \cos \frac{P\sqrt{y^2+1}}{G} - 1 \right] dy$$

Substituting from (32), and rearranging the terms, one obtains

$$T_y = e^{-P} \int_{-\infty}^{+\infty} [\cosh (Pk/G\sqrt{y^2+1}) - 1]\, dy - R_y \tag{33}$$

Making the substitution $y = \tan\theta$, the integral in (33) becomes

$$\int_{-\pi/2}^{+\pi/2} \frac{1}{\cos^2\theta} \left[\cosh \left(\frac{Pk}{G} \cos\theta \right) - 1 \right] d\theta$$

which can be shown to be equal to

$$\pi \int_0^{Pk/G} dx' \int_0^{x'} I_0(x)\, dx \tag{34a}$$

or

$$= \pi (Pk/G) \int_0^{Pk/G} I_1(x)/x\, dx \tag{34b}$$

Here $I_0(x)$ and $I_1(x)$ are the Bessel functions of imaginary argument of order zero and one respectively [$J_0(ix)$ and $J_1(ix)$]. The proof is given in Appendix I. Thus, finally,

$$T_y = \pi e^{-P} \int_0^{Pk/G} dx' \int_0^{x'} I_0(x)\, dx - R_y \tag{35}$$

$$= \pi e^{-P} \left[\int_0^{Pk/G} dx' \int_0^{x'} I_0(x)\, dx - \tfrac{1}{2} I_0(jP) + 1 - \int_0^{P/G} J_0(x)\, dx \right] \tag{36}$$

(*b*) *Asymmetrical Case, Small Absorption.*—Taking as in §5 (*b*) that $a^2G^2 \ll 1$ and $k^2 \ll 1$, we now have,

$$\sinh v = (y + iaGy)/(1 + ik) = y + i(aG - ky) \tag{37}$$

Thus,

$$\left.\begin{aligned} &\sinh v_r = y, \qquad \sin v_i = (aG - ky)/\sqrt{y^2+1} \\ &\cosh 2v_r = 1 + 2y^2, \quad \cos 2v_i = 1 \end{aligned}\right\} \tag{38}$$

to the same degree of approximation as in the last sub-section.

Also,

$$\text{Im } X = (k + aGy)/(y^2 + 1)^{\frac{1}{2}}$$

and

$$\text{Re } X = (y^2 + 1)^{\frac{1}{2}}.$$

Thus, from Eqn. (30),

$$T = \frac{e^{-P}}{2(1+y^2)} \left[\cosh \left\{\frac{P(k+aGy)}{G(y^2+1)^{\frac{1}{2}}} - 2v_r\right\} + \cos \left\{\frac{P}{G}(y^2+1)^{\frac{1}{2}} - 2v_i\right\}\right]. \quad (39)$$

The background intensity $\exp -\mu D/\gamma_0$ can be put in the form $\exp[-P(1+a)]$ and we therefore have, from Eq. (29), leaving out the odd terms:

$$T_y = e^{-P} \int_{-\infty}^{+\infty} \left[\frac{1+2y^2}{2(1+y^2)} \cosh \frac{P(k+aGy)}{G(y^2+1)^{\frac{1}{2}}} - e^{-aP} + \frac{1}{2(1+y^2)} \cos \frac{P}{G}(y^2+1)^{\frac{1}{2}} + \frac{aG}{2(1+y^2)^{3/2}} \sin \frac{P}{G}(y^2+1)^{\frac{1}{2}}\right] dy \quad (40)$$

With the help of suitable transformations, this can be put in the form:

$$T_y = e^{-P} \int_{-\pi/2}^{\pi/2} \frac{1}{\cos^2\theta} [\cosh(jP\cos\overline{\theta-\phi}) - \sin\theta \sinh(jP\cos\overline{\theta-\phi}) - e^{-aP}]\, d\theta - \frac{e^{-P}}{2} \int_{-\pi/2}^{\pi/2} \cosh(jP\cos\overline{\theta-\phi})\, d\theta + \frac{e^{-P}}{2} \int_{-\infty}^{+\infty} \frac{\cos\left(\frac{P}{G}\cosh t\right)}{\cosh t}\, dt + \frac{e^{-P}}{2} aG \int_{-\infty}^{+\infty} \frac{\sin\left(\frac{P}{G}\cosh t\right)}{\cosh^2 t}\, dt, \quad (41)$$

where $j = (a^2 + k^2G^2)^{\frac{1}{2}}$ and $\tan\phi = aG/k$ (see Appendix II). Making use of the expression for R_y from Eqn. (26), we find that the second and third terms together are exactly $= -R_y$, so that

$$T_y + R_y = e^{-P} \int_{-\pi/2}^{\pi/2} \frac{1}{\cos^2\theta} [\cosh(jP\cos\overline{\theta-\phi}) - \sin\theta\sinh(jP\cos\overline{\theta-\phi}) - e^{-aP}]\,d\theta + \frac{e^{-P}}{2} aG \int_{-\infty}^{+\infty} \sin\left(\frac{P}{G}\cosh t\right) \Big/ \cosh^2 t\,dt \qquad (42)$$

Both of these can be integrated (Appendix II) and finally we have

$$T_y + R_y = \pi e^{-P}\left[jP\int_0^{jP} I_1(x)/x\,dx + \tan\phi \text{ (integrals involving } jP \text{ and } \phi) + aG\int_0^{P/G} dx' \int_0^{x'} J_0(x)\,dx\right] \qquad (43)$$

It is readily seen that, when $a = 0$, *i.e.*, $\phi = 0$, this reduces to Eqn. (35) for the symmetrical case.

7. Variation of Integrated Reflection and Anti-Reflection with Various Factors

(*a*) *Integrated Reflection.*—The relevant formulæ are given by Eqns. (24), (25), (27) and (28). Firstly, for ordinary reflections, which are not too weak, the quantity G is usually small, of the order of 0·1 or less, so that P/G is large, for ordinary thicknesses of the order of a millimetre. Consequently, the integral is nearly equal to unity and Eqns. (27) and (36) reduce to

$$R_y = \frac{\pi}{2} e^{-P} I_0(jP) \qquad (44)$$

$$T_y = \pi e^{-P}\left[jP\int_0^{jP} I_1(x)/x\,dx - \tfrac{1}{2} I_0(jP)\right] \qquad (45)$$

Consequently, for moderate and large values of P, the integrated reflection varies as $e^{-P} I_0(jP)$. The effect of the terms left out of Eqn. (24) is to produce small fluctuations in this curve close to the origin. In fact, Eqn. (44) does not hold for small values of $P \to 0$, and the limiting value is not $\pi/2$, as would be given by this equation, but is equal to zero. This follows from the more accurate Eqn. (24), from which

$$\operatorname*{Lt}_{P\to 0} R_y = \frac{\pi}{2}\left[1 - 1 + 2\operatorname*{Lt}_{P\to 0} J_1(P/G)\right], \quad (e^P \to 1)$$
$$= \operatorname*{Lt}_{P\to 0} \pi P/G = 0.$$

This is as it should be, since a crystal of zero thickness gives no reflection.

For small P, we have

$$R_y = \frac{\pi}{2G} P e^{-P}, \tag{46}$$

which is exactly the same as that for a mosaic crystal of small thickness. In fact, if G is large, this equality of the integrated reflections of a perfect and a mosaic crystal holds over a much wider range. Eqn. (28) for a perfect crystal under these conditions is identical with the formula for a mosaic crystal (derived in Appendix III).

A large value of G signifies either that the crystal has a large absorption coefficient or that the structure amplitude of the reflection concerned is small. For a weak reflection, G is large even with medium absorption. In such a case, the formula for the integrated reflection of a perfect crystal is to be expected to be the same as that of a mosaic crystal. The reflected beam will not be allowed to build up by means of multiple reflections, owing to the heavy absorption, the beam being extinguished by absorption before the reinforcement by multiple reflections becomes effective. The mutual interaction of the incident and reflected beams throughout the bulk of the crystal, which is the essential consideration in the dynamical theory, thus ceases to be important, and it is therefore natural that the result of the more detailed dynamical theory agrees with that of the simple " kinematical " theory for a mosaic crystal.

For the same reason, even when G is not large, the result of the two theories agree for small values of P [(Eqn. (46)], *i.e.*, for small thicknesses.

(*b*) *Integrated Transmission.*—The most interesting result is that the integrated transmission may be either positive or negative, according to the conditions of the experiment. For small thicknesses, it is negative, as is to be expected from the shape of the reflection curve reported in Part I. As the thickness increases, there comes a stage, when the reflection curve contains both a dip below and a peak above the background, and the *integrated* transmission is actually zero. For larger thicknesses than this, the integrated transmission is positive.

If the incident beam is not extremely well collimated (with an angular divergence less than 1″ of arc), the variations observed in the transmitted beam would not give the true changes in intensity predicted by theory. However, a strict comparison between theory and experiment is possible by measuring the *integrated* transmission using a much wider beam for study. The formulæ in the present paper were mainly developed for this purpose and further experiments are in progress. It may be mentioned that the

formula (44) for the integrated reflection of an "internal" reflection has already been verified by Padmanabhan (1953).

8. SUMMARY

Making use of the theory developed in Part I, the integrated values of the reflected and the anti-reflected intensity have been obtained analytically for an internal reflection of a perfect crystal. Three special cases are considered, namely a symmetrical reflection, an asymmetrical reflection and also when absorption is very heavy. It is found that when absorption is large, the formula for integrated reflection reduces to that for a mosaic crystal, which may be physically explained by the fact that multiple reflections are not allowed to play a prominent part owing to the beam being quickly attenuated by absorption.

REFERENCES

1. Campbell, H. N. .. *J. Appl. Phys.*, 1951, **22**, 1139.
2. Ewald, P. B. .. *Ann. d. Phys.*, 1916, **49**, 1, 117.
3. Hirsch, P. B. and Ramachandran, G. N. *Acta Cryst.*, 1950, **3**, 187.
4. Hirsch, P. B. .. *Ibid.*, 1952, **5**, 176.
5. Laue, von M. .. *Ibid.*, 1949, **2**, 106.
6. Madelung, E. .. "*Die Mathematischen Hilfsmittel des Physikers*," Springer, Berlin, 1950, 47.
7. Padmanabhan, V. M. .. *J. Ind. Inst. Sci.*, 1953, **35**, 1.
8. Ramachandran, G. N. .. *J. Appl. Phys.*, 1952 *a*, **23**, 500.
9. ——— and Kartha, G. .. *Proc. Ind. Acad. Sci.*, 1952 *b*, **35A**, 145.
10. Watson, G. N. .. *Bessel Functions*, Cambridge, 1944, 79.
11. Zachariasen, W. H. .. *Theory of X-Ray Diffraction in Crystals*, Wiley, New York, 1945.
12. ——————— .. *Proc. Nat. Acad. Sci.*, U.S.A., 1952, **38**, 378.

APPENDIX I

Proof of Results (34 *a*) and (34 *b*)

The integral to be evaluated is

$$\int_{-\pi/2}^{\pi/2} \frac{1}{\cos^2\theta} [\cosh(q\cos\theta) - 1]\, d\theta, \tag{47}$$

where $q = jP = Pk/G$.

From the standard expressions for the Bessel function $I_0(x)$, we have

$$\pi I_0(x) = \int_{-\pi/2}^{\pi/2} \cosh(x\cos\theta)\, d\theta \tag{48}$$

Integrating this

$$\pi \int_0^{x'} I_0(x)\, dx = \int_{-\pi/2}^{\pi/2} \left[\frac{\sinh(x\cos\theta)}{\cos\theta}\right]_0^{x'} d\theta.$$

$$= \int_{-\pi/2}^{\pi/2} \frac{\sinh(x'\cos\theta)}{\cos\theta}\, d\theta \tag{49}$$

Integrating again,

$$\pi \int_0^q dx' \int_0^{x'} I_0(x)\, dx = \int_{-\pi/2}^{\pi/2} \left[\frac{\cosh(x'\cos\theta)}{\cos^2\theta}\right]_0^q d\theta$$

$$= \int_{-\pi/2}^{\pi/2} \frac{1}{\cos^2\theta} [\cosh(q\cos\theta) - 1]\, d\theta. \tag{50}$$

The right-hand side is identical with the expression (47), which proves the result (34 *a*).

We may also proceed in another manner by first integrating (47) by parts. We thus have

$$(47) = \int_{-\pi/2}^{\pi/2} \{\cosh(q\cos\theta) - 1\}\, d(\tan\theta)$$

$$= \left[\tan\theta \{\cosh(q\cos\theta) - 1\}\right]_{-\pi/2}^{\pi/2} + \int_{-\pi/2}^{\pi/2} \frac{1}{\cos\theta}\, q\sin^2\theta \sinh(q\cos\theta)\, d\theta. \tag{51}$$

The first term of (51) vanishes and since (Watson, 1944)

$$\pi\, I_1(x) = x \int_{-\pi/2}^{\pi/2} \sin^2\theta \cosh(x\cos\theta)\, d\theta,$$

the second term is equal to

$$\pi q \int_0^a I_1(x)/x\, dx, \tag{52}$$

which is the result (34 *b*).

APPENDIX II

Simplification of the Integrals in Eqn. (42)

The integral to be evaluated is

$$\int_{-\pi/2}^{\pi/2} \frac{1}{\cos^2\theta} [\cosh(jP\cos\overline{\theta-\phi}) - \sin\theta \sinh(jP\cos\overline{\theta-\phi}) - e^{-aP}]\, d\theta \tag{53}$$

where $j\sin\phi = a$. This may be written in the form

$$\int_{-\frac{\pi}{2}-\phi}^{\frac{\pi}{2}-\phi} \sec^2(\theta+\phi)\,[\cosh(jP\cos\theta) - \sin(\theta+\phi)\sinh(jP\cos\theta) - e^{-aP}]\, d\theta \tag{54}$$

Integrating by parts as in the previous Appendix I, we obtain

$$\Big[\tan(\theta+\phi)\cosh(jP\cos\theta) - \sec(\theta+\phi)\sinh(jP\cos\theta) - e^{-aP}\Big]_{-\frac{\pi}{2}-\phi}^{\frac{\pi}{2}-\phi}$$

$$+ \int_{-\frac{\pi}{2}-\phi}^{\frac{\pi}{2}-\phi} \tan(\theta+\phi)\, jP\sin\theta\sinh(jP\cos\theta)\, d\theta$$

$$- \int_{-\frac{\pi}{2}-\phi}^{\frac{\pi}{2}-\phi} \sec(\theta+\phi)\, jP\sin\theta\cosh(jP\cos\theta)\, d\theta.$$

The first term is again equal to zero, and making the substitutions

$$\tan(\theta+\phi) = \tan\theta + \tan\phi + \tan\theta\tan\phi\tan(\theta+\phi) \tag{56}$$

and $$\sec(\theta+\phi) = \sec\theta\sec\phi + \tan\theta\tan\phi\sec(\theta+\phi) \tag{57}$$

in (55) and putting $jP = q$, we get the integral (53) as

$$\int_{-\frac{\pi}{2}-\phi}^{\frac{\pi}{2}-\phi} (q/\cos\theta)\sin^2\theta \sinh(q\cos\theta)d\theta$$
$$+ \int q \tan\phi \sin\theta \sinh(q\cos\theta)\, d\theta$$
$$+ \int q \tan\phi (\sin^2\theta/\cos\theta) \tan(\theta+\phi) \sinh(q\cos\theta)\, d\theta$$
$$- \int q \sec\phi \tan\theta \cosh(q\cos\theta)\, d\theta$$
$$- \int q \tan\phi (\sin^2\theta/\cos\theta) \sec(\theta+\phi) \cosh(q\cos\theta)\, d\theta \qquad (58)$$

The second and the fourth terms vanish, and the first term can be shown to be equal to (52), so that we finally obtain the integral (53) in the form

$$\pi jP \int_0^{jP} I_1(x)/x\, dx$$
$$+ \tan\phi \left[\int_{-\frac{\pi}{2}-\phi}^{\frac{\pi}{2}-\phi} jP (\sin^2\theta/\cos\theta) \tan(\theta+\phi) \sinh(jP\cos\theta)\, d\theta \right.$$
$$\left. - \int_{-\frac{\pi}{2}-\phi}^{\frac{\pi}{2}-\phi} jP (\sin^2\theta/\cos\theta) \sec(\theta+\phi) \cosh(jP\cos\theta)\, d\theta \right] \qquad (59)$$

APPENDIX III

Derivation of R_y for an Internal Reflection given by a Mosaic Crystal

If Q stands for the well-known expression

$$Q = \frac{C}{\sin 2\theta_B} \frac{e^4}{m^2c^4} \lambda^3 F^2 N^2 \quad (C = 1 \text{ or } \cos^2\theta) \qquad (60)$$

and D is the thickness of the crystal slab, then the integrated reflection for the whole crystal is

$$\int_0^D \frac{Q}{\gamma_0} \exp\left[-\frac{\mu x}{\gamma_0} - \frac{\mu(D-x)}{\gamma_h}\right] dx$$
$$= \frac{Q}{\mu(1-\gamma_0/\gamma_h)} \exp\left[-\frac{\mu D}{2}\left(\frac{1}{\gamma_0}+\frac{1}{\gamma_h}\right)\right] \cdot 2\sinh\left[\frac{\mu D}{2}\left(\frac{1}{\gamma_0}-\frac{1}{\gamma_h}\right)\right] \qquad (61)$$

Putting $\frac{\mu D}{2}\left(\frac{1}{\gamma_0}+\frac{1}{\gamma_h}\right)=P$ and $(1-b)/(1+b)=a$ (the asymmetry factor), this becomes

$$=\frac{2Q}{\mu(1+b)}e^{-P}\frac{\sinh aP}{a} \tag{62}$$

Converting into the y-scale, we have

$$R_y(\text{mosaic})=\frac{\pi}{2G}e^{-P}\frac{\sinh aP}{a} \tag{63}$$

THE INFRA-RED ABSORPTION SPECTRUM OF BARYTES

By A. K. Ramdas

(*Memoir No. 47 of the Raman Research Institute, Bangalore*)

Received February 4, 1954

(Communicated by Sir C. V. Raman)

1. Introduction

Though the Raman spectrum of barytes has been studied in detail by many workers, in particular by R. S. Krishnan[1] and L. Couture,[2] the infra-red absorption studies have remained inadequate. The earlier works have been those of Coblentz,[3], Schæfer and Schubert,[4] and Matossi and Kindler[5] in the short wavelengths from 2μ to 16μ by absorption and reflexion methods; and of Liebisch and Rubens[6] in the far infra-red upto 300μ by reflexion method. The present author has reinvestigated the infra-red spectra of barytes by transmission in the range 1μ to $25{\cdot}5\mu$. In this paper it is proposed to present the experimental results obtained by the author and discuss them in the light of selection rules and the Raman effect data.

2. Experimental Results

The crystals of barytes were examined in the 001 and 110 cleavage sections. A Beckman infra-red spectrophotometer provided with KBr-optics was used to measure the percentage transmission at $0{\cdot}05\mu$ intervals and at still closer intervals near absorption maxima. Ten specimens of different thicknesses were examined. We reproduce in Figs. 1, 2 and 3, the infra-red spectra (% cut-off *vs.* $\lambda\mu$) of three specimens showing all the features in the clearest manner. (Fig. 1: Specimen VI, 001 section, thickness 1·7 mm.; Fig. 2: Specimen VII, 001 section, thickness 3·0 mm.; Fig. 3: Specimen VIII, 110 section, thickness 0·25 mm.) The following features are noticed.

I. Numerous very weak absorption maxima are exhibited between 1μ and 4μ, *viz.*, at $2{\cdot}5\mu$, 3μ, $3{\cdot}3\mu$ and $3{\cdot}5\mu$ for specimen VI; at $2{\cdot}5\mu$, 3μ, $3{\cdot}3\mu$ and $3{\cdot}7\mu$ for specimen VII; at $2{\cdot}5\mu$, 3μ, $3{\cdot}3\mu$, $3{\cdot}5\mu$ and at $3{\cdot}7\mu$ for specimen VIII. Of these the $3{\cdot}3\mu$ absorption maximum is the strongest and is brought out best in Fig. 2. Matossi and Kindler found additional bands at $2{\cdot}35\mu$, $2{\cdot}41\mu$, $2{\cdot}66\mu$, $3{\cdot}19\mu$, $3{\cdot}8\mu$ and $3{\cdot}9\mu$. Coblentz reported the one at $3{\cdot}0\mu$.

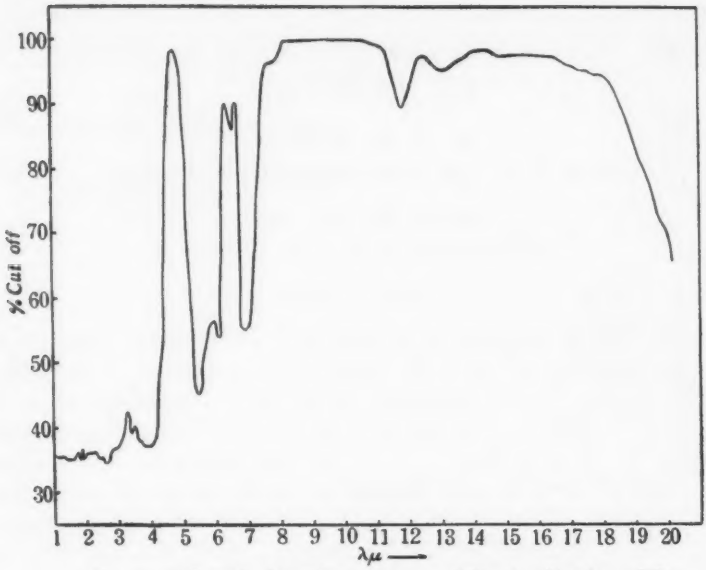

FIG. 1. Infra-red absorption spectrum of barytes (Specimen VI)

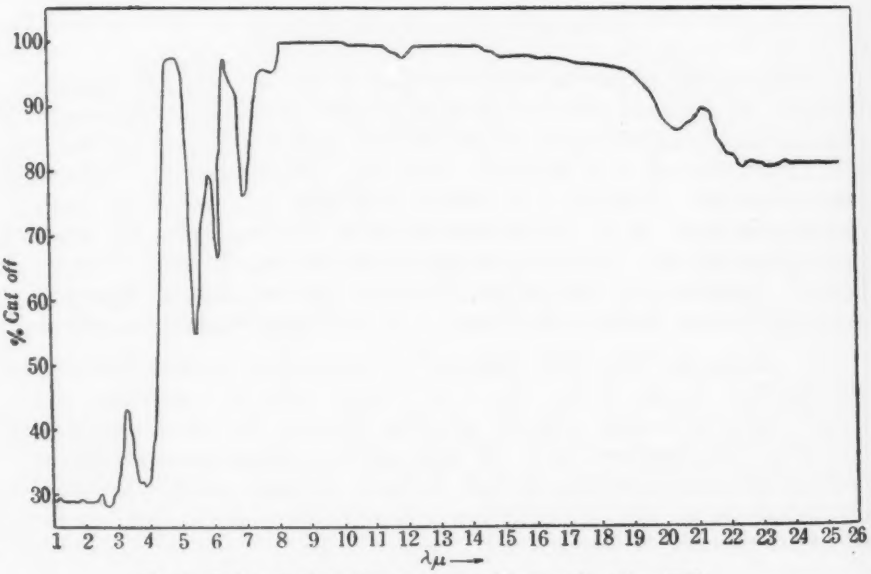

FIG 2. Infra-red absorption spectrum of barytes (Specimen VII)

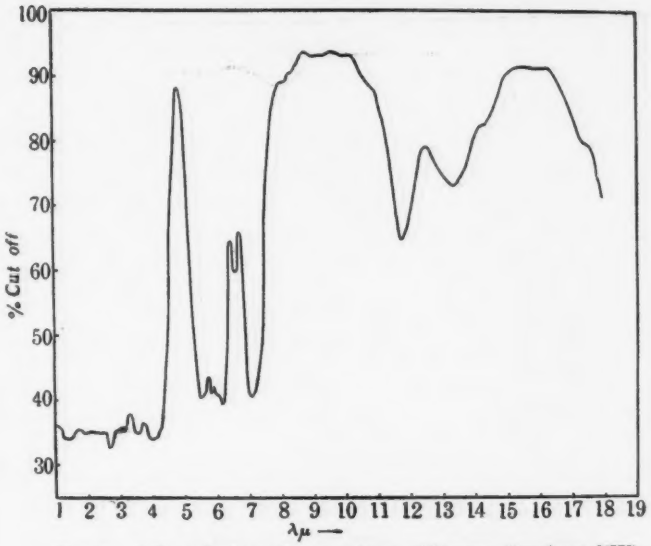

FIG. 3. Infra-red absorption spectrum of barytes (Specimen VIII)

II. The region between 4μ and 7μ shows intense and well defined absorption maxima. Fig. 1 shows a sharply defined band at $4{\cdot}8\mu$ with a companion at $4{\cdot}9\mu$, a weak one at $5{\cdot}9\mu$, an intense doublet at $6{\cdot}4\mu$ and $6{\cdot}7\mu$. Fig. 2 shows a slightly broad band between $4{\cdot}7\mu$ to $4{\cdot}9\mu$; the $5{\cdot}9\mu$ band is rather strong and well brought out, while instead of a well resolved doublet $6{\cdot}4\mu$ and $6{\cdot}7\mu$, a maximum at $6{\cdot}4\mu$ and an inflexion at $6{\cdot}7\mu$ are observed. This is due to the greater thickness of specimen VII. In Fig. 3, bands at $4{\cdot}9\mu$ (intense), $5{\cdot}75\mu$, $5{\cdot}85\mu$ (very weak), and a well resolved doublet $6{\cdot}4\mu$ and $6{\cdot}7\mu$, the latter being the stronger band. These differences observed between specimens VI and VII on the one hand and specimen VIII on the other are evidently connected with the fact that the former are 001 sections and the latter is a 110 section. In this range Matossi and Kindler reported the following maxima: $4{\cdot}32\mu$, $4{\cdot}61\mu$, $4{\cdot}82\mu$, $5{\cdot}12\mu$, $5{\cdot}87\mu$, $6{\cdot}27\mu$, $6{\cdot}51\mu$ and $6{\cdot}99\mu$; Coblentz observed bands at $4{\cdot}6\mu$, $6{\cdot}2\mu$ and $6{\cdot}5\mu$.

III. The region from 7μ to 12μ is one of intense cut-off. Reflexion studies of Coblentz and of Schæfer and Schubert reveal reststrahlen maxima at $8{\cdot}3\mu$, $8{\cdot}93\mu$ and $9{\cdot}1\mu$ indicating the presence of fundamentals. Observations with polarised light and orientational studies show that these reflexion maxima are polarised along the *a*, *b* and *c* axes of the crystal. Figs. 1 and 2 exhibit strong cut-off between 8μ and 11μ. In Fig. 3 there are indications

of resolution of this strong band into several maxima such as those at $8{\cdot}3\,\mu$, $8{\cdot}8\,\mu$, $9{\cdot}6\,\mu$ and $10{\cdot}2\,\mu$, with an inflexion at $10{\cdot}8\,\mu$.

IV. We notice a rather broad absorption from $12{\cdot}3\,\mu$ to $14{\cdot}4\,\mu$ in Fig. 2, while a well defined maximum at $12{\cdot}55\,\mu$ replaces it in both Figs. 1 and 3. In Fig. 1, beyond this, a maximum at $14{\cdot}4\,\mu$ is seen followed by constant and strong absorption region right upto $16{\cdot}6\,\mu$. Thereafter it shows a rapid fall upto $20{\cdot}2\,\mu$. No observations could be made with this specimen beyond $20{\cdot}2\,\mu$ as its area was too small for accurate measurements. In Fig. 2, there is almost total cut-off from $15\,\mu$ to $19\,\mu$. From $19\,\mu$ onwards a slow falling off is seen, and at $21{\cdot}3\,\mu$ a well defined maximum has been obtained, with hints of maxima at $22{\cdot}2\,\mu$, $22{\cdot}8\,\mu$ and $23{\cdot}8\,\mu$. The very large area of specimen VII has enabled observations to be made right upto $25{\cdot}5\,\mu$, the limit of the instrument employed in the present work. It appears that the above maxima beyond $20\,\mu$ have been observed for the first time. In Fig. 3, an inflexion at $14{\cdot}4\,\mu$ is noticed and, instead of the strong cut-off seen in the other figures, a comparatively narrower band between $15\,\mu$ to $16{\cdot}4\,\mu$ is seen, with definite indications of maxima at $15{\cdot}6\,\mu$, $15{\cdot}8\,\mu$ and $16{\cdot}3\,\mu$. Matossi and Kindler obtained maxima at $12{\cdot}35\,\mu$ and $15{\cdot}65\,\mu$. Schæfer and Schubert report a reflexion maximum at $15{\cdot}8\,\mu$.

3. THEORETICAL CONSIDERATIONS

Barytes belongs to the space group V_h^{16} (Pnma) with four molecules of $BaSO_4$ per unit cell. The vibrations of barytes can be divided into two classes: (1) low frequency lattice oscillations in which SO_4 molecules move as units against Ba atoms, and (2) high frequency oscillations which constitute internal movements of the atoms comprising the SO_4 molecule. In the range studied in this investigation, we may expect (as we shall see presently) only the high frequency oscillations, internal to SO_4 molecules to appear as fundamentals.

The free SO_4 molecule belongs to the T_d symmetry. Accordingly it possesses four fundamental vibrations: totally symmetric $\nu_1\,(A_1)$; doubly degenerate $\nu_2\,(E)$; and triply degenerate $\nu_3\,(F_2)$ and $\nu_4\,(F_2)$. All of these are Raman active, but only the F_2-type vibrations are infra-red active.

Corresponding to each of the vibration of the free SO_4 molecule, one expects to find a number of vibrations in the crystalline state. The number and their respective symmetry properties can be found out according to the procedure outlined by Couture and Mathieu.[7] The effect of the crystalline state on the free SO_4 oscillations is two-fold. The symmetry of a single SO_4 molecule is changed from the tetrahedral group T_d to the monoclinic

local symmetry C_s, lifting the degeneracies of the doubly and triply degenerate oscillations; in this manner the *four* fundamentals of the free SO_4 molecule give *nine* fundamentals. A further increase in the modes of vibrations is brought about by the coupled oscillations of the four SO_4 molecules in the unit cell; in this way the above nine fundamentals multiply to yield a total of *thirty-six* internal vibrations of the barytes crystal. The transformation of the vibrations of the free SO_4 molecule into the internal modes of barytes can be pictured as given in Table I.

TABLE I

Free SO_4 molecule $\rightarrow$ (T_d)	Local symmetry $\rightarrow$ (C_s)	Unit cell symmetry (V_h)
$\nu_1(A_1) \longrightarrow$	ν_1^1 (A′)	ν_1^1 (A_{1g}), ν_1^2 (B_{2g}), ω_1^1 (B_{1u}), ω_1^2 (B_{3u})
$\nu_2(E) \longrightarrow$	ν_2^1 (A′)	ν_2^1 (A_{1g}), ν_2^2 (B_{2g}), ω_2^3 (B_{1u}), ω_2^4 (B_{3u})
	ν_2^2 (A″)	ν_2^3 (B_{1g}), ν_2^4 (B_{3g}), ω_2^1 (A_{1u}), ω_2^2 (B_{2u})
$\nu_3(F_2) \longrightarrow$	ν_3^1 (A′)	ν_3^1 (A_{1g}), ν_3^3 (B_{2g}), ω_3^1 (B_{1u}), ω_3^2 (B_{3u})
	ν_3^2 (A′)	ν_3^2 (A_{1g}), ν_3^4 (B_{2g}), ω_3^3 (B_{1u}), ω_3^4 (B_{3u})
	ν_3^3 (A″)	ν_3^5 (B_{1g}), ν_3^6 (B_{3g}), ω_3^5 (A_{1u}), ω_3^6 (B_{2u})
$\nu_4(F_2) \longrightarrow$	ν_4^1 (A′)	ν_4^1 (A_{1g}), ν_4^3 (B_{2g}), ω_4^1 (B_{1u}), ω_4^2 (B_{3u})
	ν_4^2 (A′)	ν_4^2 (A_{1g}), ν_4^4 (B_{2g}), ω_4^3 (B_{1u}), ω_4^4 (B_{3u})
	ν_4^3 (A″)	ν_4^5 (B_{1g}), ν_4^6 (B_{3g}), ω_4^5 (A_{1u}), ω_4^6 (B_{2u})

Selection rules show that: for T_d, all are Raman active but only F_2's are infra-red active; for C_s, all are Raman and infra-red active; for V_h, all *g*'s are Raman active, infra-red inactive, all *u*'s are infra-red active, Raman inactive, with the exception of A_{1u}'s which are inactive in both. The ν's are Raman active, and the ω's infra-red active, the two sets being mutually exclusive because of the presence of centre of inversion. Further, the infra-red vibrations are polarised along *a* (B_{3u}), *b* (B_{2u}) or *c* (B_{1u}) axes of the crystal.

Hence under favourable conditions one should be able to observe eighteen Raman lines and fifteen infra-red lines corresponding to the internal modes of SO_4 in barytes.

4. Discussion of Results

The four fundamentals of the free SO_4 molecule from studies of Raman effect in the liquid state are found to be: 980 cm.$^{-1}$ [ν_1 (A_1)], 450 cm.$^{-1}$ [ν_2 (E)], 620 cm.$^{-1}$ [ν_3 (F_2)] and 1100 cm.$^{-1}$ [ν_4 (F_2)]. According to the analysis given above eighteen Raman lines and fifteen infra-red lines of the

internal type should be observed in the proximity of these frequencies, falling into four groups as indicated. The two sets are mutually exclusive.

Couture[2] has been able to discover thirteen internal fundamental Raman lines and give them proper assignments, by a detailed investigation of their depolarisation values with directional excitation.

The infra-red active fundamentals corresponding to $\nu_4(F_2)$, expected in the neighbourhood of 1100 cm.$^{-1}$ lie in a region of intense cut-off. The reflexion studies, however, give three maxima at 8·3 μ, 8·93 μ and 9·1 μ, and according to their polarisations one can ascribe to them B_{3u}, B_{2u} and B_{1u} types respectively. In the present studies we get maxima at 8·3 μ, 8·8 μ and 9·6 μ with 110 section. The former two are presumably the same as 8·3 μ and 8·93 μ reflexion maxima while 9·6 μ appears to be a weak B_{3u} type of vibration. We have entered them as the infra-red active fundamentals in Table II.

The infra-red fundamental corresponding to $\nu_1(A_1)$ is taken as the one at 10·2 μ observed in the present study. The $\nu_1(A_1)$ is a totally symmetric infra-red inactive, Raman-active vibration. The infra-red activity which the corresponding vibrations in the crystalline state acquire will be as a result of the distortion caused by the crystalline state. Barytes is weakly birefringent ($N_g - N_p = 0{\cdot}012$) and thus, though qualitatively allowed to appear on symmetry considerations alone, quantitatively the vibrations may appear only weakly. However, these can be expected to appear with great intensity in Raman effect, especially the totally symmetric one. The most intense Raman line observed by Krishnan is the one at 988·6 cm.$^{-1}$ (A_{1g}). Another Raman line at 967 cm.$^{-1}$ has been observed by Krishnan which he describes as ' the most intense one (of the 2nd order lines) as it appears even in the lightly exposed photograph '. It has not been possible to identify it as an overtone or a combination. This is highly suggestive of its being the $\nu_1^2(B_{2g})$ vibration.

Similar remarks as to the activity of the infra-red vibrations corresponding to $\nu_2(E)$ can be made. We have observed in the present work fairly strong and sharp maximum at 21·3 μ (469·5 cm.$^{-1}$) and a rather weak one at 22·8 μ (439 cm.$^{-1}$) using a very thick crystal. These have been observed with 001 section and hence must belong to B_{2u} or B_{1u} symmetry. Polarisation studies must be made to decide to which of them they actually belong. The Raman lines at 453 cm.$^{-1}$ and 462 cm.$^{-1}$ are among the most intense Raman lines observed by Krishnan.

The knowledge of the infra-red active fundamentals representing $\nu_3(F_2)$ in the crystal is perhaps the least. Theoretically, five vibrations are expected,

three in the 001 section and all the five in the 110 section. Reflexion studies have yielded but one at $15{\cdot}8\,\mu$ with 001 section and the present work three at $15{\cdot}6\,\mu$, $15{\cdot}8\,\mu$ and $16{\cdot}3\,\mu$ with 110 section. Nothing is known about their polarisation properties.

The Raman active and the infra-red active internal oscillations of barytes which can be derived from the data available can be summarised as in Table II.

TABLE II

Raman active	Infra-red active	Raman active	Infra-red active
$\nu_1^1(A_{1g}) = 988$ cm.$^{-1}$	$\omega_1^1(B_{1u})$ } 980 cm.$^{-1}$	$\nu_3^1(A_{1g}) = 622$ cm.$^{-1}$	$\omega_3^1(B_{1u})$ } 641 cm.$^{-1}$
$\nu_1^2(B_{2g}) = 967$	$\omega_1^2(B_{3u})$ }	$\nu_3^2(A_{1g}) = 630$	$\omega_3^2(B_{3u})$
		$\nu_3^3(B_{2g}) = ?$	$\omega_3^3(B_{1u})$ } 633 ,,
$\nu_2^1(A_{1g}) = 453$	..	$\nu_3^4(B_{2g}) = 647$	$\omega_3^4(B_{3u})$ } 614 ,,
$\nu_2^2(B_{2g}) = 453$	$\omega_2^2(B_{2u}$ or $B_{1u}) = 439$	$\nu_3^5(B_{1g}) = —?$	..
$\nu_2^3(B_{1g}) = 462$	$\omega_2^3(B_{1u}$ or $B_{2u}) = 470$	$\nu_3^6(B_{3g}) = 622$	$\omega_3^6(B_{2u})$ }
$\nu_2^4(B_{3g}) = —?$	$\omega_2^4(B_{3u}) = — ?$	$\nu_4^1(A_{1g}) = 1105$	$\omega_4^1(B_{1u}) = 1136$
		$\nu_4^2(A_{1g}) = 1145$	$\omega_4^2(B_{3u}) = 1042$
		$\nu_4^3(B_{2g}) = 1138$	$\omega_4^3(B_{1u}) = —$
		$\nu_4^4(B_{2g}) = 1167$	$\omega_4^4(B_{3u}) = 1205$
		$\nu_4^5(B_{1g}) = —?$	..
		$\nu_4^6(B_{3g}) = 1084$	$\omega_4^6(B_{2u}) = 1100$

As described in the experimental part of the paper, there are several absorption maxima in the wavelengths below $8\,\mu$. These will naturally find explanation only as harmonics of the fundamentals. Selection rules show that they too will be polarised along the axes *a*, *b* or *c*. Hence to give them proper assignments, their polarisations should be considered. Matossi and Kindler have given assignments to these higher order absorption maxima on the basis of the four fundamentals of the free SO_4 molecule. As the theory predicts and the experiments confirm, one has to explain the infra-red and Raman spectra on the basis of vibrations of the four SO_4 molecules contained in the unit cell of the crystal. Even with the incomplete knowledge of the fundamentals, it is possible to give satisfactory assignments to the entire body of data (Table III). When the remaining unknown fundamentals

TABLE III

Observed			Assignment	Calculated
λμ	cm.$^{-1}$	Section		cm.$^{-1}$
2·35	4255	001	..	
2·41	4149	,,	$2\nu_4^2+\nu_3^4+\omega_4^4$	4142
2·5	4000	,,+110	$2\nu_4^6+\omega_4^4+\nu_3^2$ $2\nu_4^4+\omega_4^2+\nu_3^1(\nu_3^6)$ $2\nu_4^3+\omega_4^6+\nu_3^1(\nu_3^6)$	4003 3998 3998
2·66	3759	,,	$3\omega_4^6+\nu_2^1(\nu_2^2)$	3753
3·0	3333	,,+110	$2\nu_4^2+\omega_4^2$	3332
3·2	3125	,,	$3\omega_4^2$	3126
3·3	3030	,,+110	$2\nu_1^1+\omega_4^2$	3018
3·5	2857	,,+110	$\nu_4^1+\nu_3^4+\omega_4^6$	2852
3·7	2703	,,+110	$\nu_4^2+\omega_4^6+\nu_2^1(\nu_2^2)$	2698
3·8	2632	,,	$\nu_4^6+\omega_4^6+\nu_2^1(\nu_2^2)$	2637
3·9	2564	,,	$\nu_4^3+\omega_1^1+\nu_2^1(\nu_2^2)$	2571
4·32	2315	,,	$2\nu_3^2+\omega_4^2$	2302
4·61	2169	,,	$\nu_1^2+\omega_4^4$	2172
4·7	2128	,,	$\nu_4^6+\omega_4^2$, $\nu_4^1+\omega_1^1$, $\nu_1^1+\omega_4^6$, $\nu_4^6+\omega_1^1$, $\nu_4^3+\omega_1^1$	2126, 2085, 2088, 2064, 2118
↓	↓			
4·9	2041			
4·8	2083	,,	$\omega_1^1+\nu_4^1$, $\nu_1^1+\omega_4^6$	2085, 2088
4·9	2041	110	$\nu_1^1+\omega_4^2$	2030
5·12	1953	001	$\nu_1^2+\omega_1^1$	1947
5·75	1739	110	$\nu_3^2+\omega_4^6$	1730
5·85	1709	,,	..	
5·9	1695	001	..	
6·27	1595	,,	$\nu_3^1+\omega_1^1$, $\nu_3^6+\omega_1^1$	1602
6·4	1562	,,	$\nu_2^3+\omega_4^6$	1562
6·51	1536	,,	$\nu_4^1+\omega_2^2$	1544
6·7	1493	,,	$\nu_2^1+\omega_4^2$, $\nu_2^2+\omega_4^2$	1495
6·99	1431	,,	$\nu_2^1+\omega_1^1$, $\nu_2^2+\omega_1^1$	1433
7·8	1282	,,	$\nu_3^4+\omega_3(=633)$	1280
8·3	1203		ω_4^4	
8·8	1136		ω_4^1	
9·1	1100		ω_4^6	
9·6	1042		ω_4^2	
10·2	980	110	ω_1^1	
10·8	926	,,	$\nu_2^1+\omega_2^3$	923
12·35	810	001	ν_3^4+164	811
12·55	796	,,+110	ν_3^2+164	794
14·4	694·4	,,	ν_3^1+77	699
15·6 15·8 16·3	641 633 614	110	ω_3's	
21·3	470	001	ω_2^3	
22·2	451	,,	..	
22·8	439	,,	ω_2^2	
23·8	420	,,	..	

are also discovered, and accurate polarisation studies are made the assignments given in Table III, may have to be revised.

The extreme infra-red studies of Liebisch and Rubens already referred to, revealed the existence of low frequency infra-red fundamentals at 103 cm.$^{-1}$, 161 cm.$^{-1}$ (B_{1u}); at 83 cm.$^{-1}$, 164 cm.$^{-1}$ (B_{2u}); at 77 cm.$^{-1}$, $\sim$140 cm.$^{-1}$

and 196 cm.$^{-1}$ (B_{3u}). The Raman spectra have given lines at 67 cm.$^{-1}$ (A_{1g}), 77 cm.$^{-1}$ (A_{1g}), 92 cm.$^{-1}$ (B_{2g}), 131 cm.$^{-1}$ (A_{1g} ?), 149 cm.$^{-1}$(B_{3g}) and 193 cm.$^{-1}$ (B_{2g}, A_{1g} ?) according to Couture and in addition at 58·5 cm.$^{-1}$, 88·3 cm.$^{-1}$ and 151·4 cm.$^{-1}$ according to Krishnan. All these are low frequency lattice oscillations. According to group theoretical analysis, eighteen Raman active—infra-red inactive, eleven infra-red active—Raman inactive, and four inactive in both—thus in all thirty-three lattice oscillations are expected. These naturally lie beyond the range studied in this investigation, but combinations between internal and lattice vibrations may appear when allowed to do so by selection rules. An interpretation on this basis has been given in Table III in a few cases, where no other assignment is possible.

In conclusion, I wish to express my best thanks to Professor Sir C. V. Raman for the encouragement and guidance he gave me during this investigation.

5. Summary

The infra-red absorption spectrum of barytes has been studied in the range 1 μ to 25 μ using ten different specimens, belonging to 001 and 110 sections. The extension of the range of study beyond 16 μ has revealed the presence of fundamentals at 21·3 μ (470 cm.$^{-1}$) and 22·8 μ (439 cm.$^{-1}$) besides other absorption maxima. The review of the available data shows that of the eighteen Raman active internal oscillations of barytes, fourteen can be identified including the one at 967 cm.$^{-1}$ not previously recognised as such. The infra-red studies give ten of the fifteen theoretically possible infra-red active internal oscillations. The numerous absorption bands observed in the range studied find satisfactory explanation in terms of the infra-red active fundamentals in conjunction with the Raman active ones, applying selection rules appropriate to the unit cell of the crystal.

References

1. Krishnan .. *Proc. Ind. Acad. Sci.*, 1946, **23A**, 288.
2. Couture .. *Annales de Physique*, 1947, **2**, 5.
3. Coblentz .. *Investigations of Infra-red Spectra*, Carnegie Institution of Washington, 1906, 53, 78.
4. Schæfer and Schubert . *Ann. der. Phys.*, 1916, **50**, 283.
5. Matossi and Kindler .. *Zeit. für. Phys.*, 1934, **92**, 303.
6. Liebisch and Rubens .. *Sitz. Preuss. Akad. Wiss.*, 1919, **12**, 198.
7. Couture and Mathieu .. *J. Phy. Rad.*, 1949, **10**, 145.

SYNTHETICAL EXPERIMENTS IN THE CHROMONE GROUP

Part XXX. A Synthesis of 3 : 5 : 8 : 3′ : 4′-Pentahydroxyflavone and Its Non-identity with Ponderosin

By V. Ramanathan and K. Venkataraman, F.A.Sc.

(Department of Chemical Technology, University of Bombay)

Received January 4, 1954

Kurth and Hubbard[1] isolated from *Ponderosa* pine bark a bright yellow colouring matter, to which we propose to assign the name ponderosin. It was soluble in acetone and alcohol, slightly soluble in water and insoluble in benzene, hexane and ethyl acetate; crystallization from acetone, ether and alcohol gave a material melting at 305–07° with decomposition. Reduction with magnesium and hydrochloric acid gave a pink colour and the test with Wilson's boric acid reagent[2] was positive. Molecular weight determination by the ebullioscopic method in ethyl alcohol gave values of 305 and 314, and the elementary analysis corresponded to $C_{15}H_{10}O_7$. A pentacetate with a m.p. of 237–39° was obtained on treatment with acetic anhydride and sodium acetate. The pentamethyl ether, m.p. 198–99°, was prepared by methylation with diazomethane in dry ether containing a trace of methanol till the methoxyl content did not increase; the product was insoluble in aqueous caustic soda and gave no colour with ferric chloride. Oxidation of the pentamethyl ether with hot alkaline potassium permanganate gave veratric acid. Fusion of ponderosin with caustic potash and methylation of the products with dimethyl sulphate gave veratrole and 1 : 2 : 4-trimethoxybenzene. Ponderosin thus appeared to be one of three pentahydroxyflavones: 3 : 5 : 6 : 3′ : 4′ (I), 3 : 6 : 7 : 3′ : 4′ (II), or 3 : 5 : 8 : 3′ : 4′ (III).

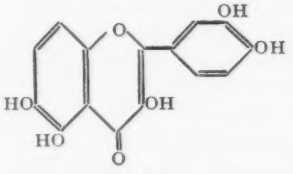

(I)

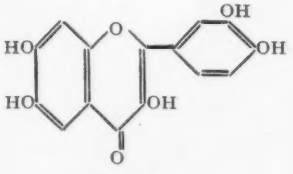

(II)

The structure (III) was then assigned, since (I) and (II) synthesized by Row and Seshadri[3] had properties different from those of ponderosin; (II) was

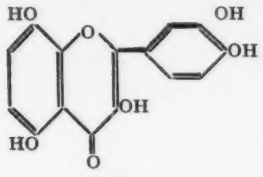

(III)

also ruled out because a positive Wilson's boric acid test indicates a 5-hydroxyl group in a flavone.

3 : 5 : 8 : 3′ : 4′-Pentahydroxyflavone (III) has now been synthesized and found to be different from ponderosin by a direct comparison. The properties of the pentahydroxyflavones (I), (II), (III) and ponderosin are shown in Table I.

In the course of our studies in Raney nickel reductions[4] a method[5] was developed for reducing 5 : 7-dihydroxyflavones to 5-hydroxyflavones by the action of Raney nickel and hydrogen on the 7-tosyl ester (*cf.* Kenner and Murray).[6] This reaction has many interesting synthetic possibilities and has now been used for the synthesis of the flavone (III). 5 : 7-Dihydroxy-3 : 3′ : 4′-trimethoxyflavone (IV)[7] readily gave the 7-tosyl ester (V) on treatment with a molar proportion of *p*-toluenesulphonyl chloride and anhydrous potassium carbonate in boiling acetone. The hydrogenolysis of this derivative (V) with Raney nickel and hydrogen was carried out under controlled conditions leaving a part of the tosyl derivative unreacted in order to avoid reduction beyond the desired stage. The crude reaction product was

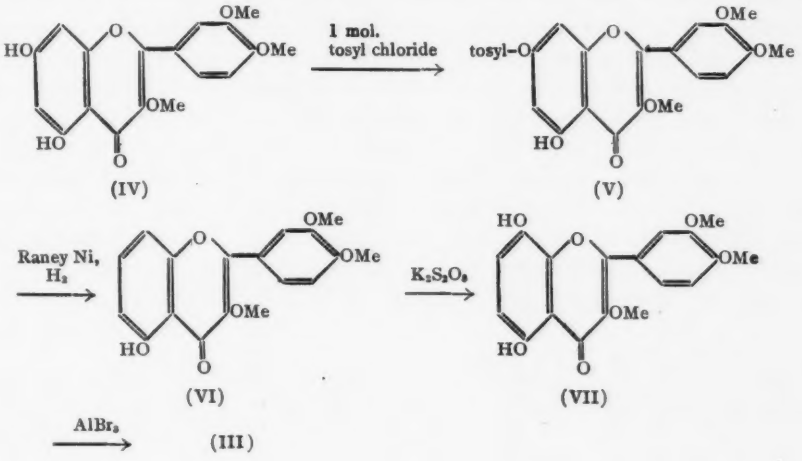

TABLE I

Properties of 3:5:6:3′:4′-, 3:6:7:3′:4′-, *and* 3:5:8:3′:4′-*pentahydroxyflavones and of ponderosin*

Pentahydroxy-flavone	m.p. ° C.	Fluorescence in alcoholic solution	Colour in aqueous caustic soda	Colour in potassium carbonate solution	Colour in concentrated sulphuric acid	Ferric chloride colouration	Lead acetate	M.P. of pentacetate ° C.	M.P. of pentamethyl ether ° C.
3:5:6:3′:4′	Sinters 310 318–20	None			Bright yellow, no fluo-rescence	Dark olive green		196	121–2
3:6:7:3′:4	Does not melt below 310, darkens 315–20	Bright green	Bright stable orange-yellow		Bright yellow, green fluo-rescence	Dark olive green	Heavy orange-red preci-pitate	223–4	186–7
3:5:8:3′:4′	270–71	None	Yellow-orange, turning pink	Yellow-orange, turning pink	Bright yellow, no fluo-rescence	Dark green	Heavy orange-red preci-pitate	236–7	155
Ponderosin	305–07		Green	Dark green	Bright orange	Dark green	Orange colouration	237–9	198–99 (diazomethane) 173 (dimethyl sulphate)

treated with alcoholic caustic potash to hydrolyse the unreacted tosyl derivative. From the resulting mixture of hydroxyflavones (IV and VI), 5-hydroxy-3 : 3′ : 4′- trimethoxyflavone (VI) was extracted with cold benzene and purified further by chromatography on Florex. Oxidation of (VI) with potassium persulphate according to Rao and Seshadri[8] yielded 5 : 8-dihydroxy-3 : 3′ : 4′-trimethoxyflavone (VII).

Demethylation of the trimethyl ether (VII) with hydriodic acid gave a product which melted over a range and was difficult to crystallize. Aluminium chloride as a demethylating agent is free from the complication of rearrangement of flavones with hydroxyl groups in the 5 : 8-positions to the corresponding 5 : 6-compounds.[9] Briggs and Locker[10] found in connection with their work on meliternatin that, when aluminium chloride in nitrobenzene at 100° was used as the dealkylating agent, an aluminium lake was formed from which the metal could not be removed. Under milder conditions, using aluminium chloride in boiling ether, only partial dealkylation took place with the formation of a flavonol still containing one methoxyl group and giving a positive methylenedioxy test. Seshadri and co-workers[11] have reported failure in their attempt to demethylate " the higher members of the norwogonin series " with aluminium chloride. By using aluminium bromide which is readily soluble in benzene, the ether (VII) has now been smoothly demethylated to the pentahydroxy compound (III). The 5 : 8-orientation of the hydroxyl groups in the fused benzene ring was shown by the positive gossypetone reaction. The pentahydroxyflavone (III) dissolved in 0·1 N caustic soda and in potassium carbonate solution to yellow-orange solutions changing to pink, unlike ponderosin which gave a green colour with these reagents; (III) was soluble in ethyl acetate unlike ponderosin. The m.p. of (III) was depressed by mixing with ponderosin. Acetylation of (III) with acetic anhydride and pyridine gave the pentacetate, m.p. 236–37° which was depressed to 210–12° on admixture with the pentacetate prepared from ponderosin. The pentamethyl ether obtained by treatment of (VII) with dimethyl sulphate and anhydrous potassium carbonate in boiling acetone melted at 155°. For the purpose of comparison, ponderosin was methylated by the same method and the pentamethyl ether had m.p. 173°, while the product obtained by Kurth and Hubbard by means of diazomethane melted at 198–99°.

3 : 5 : 8 : 3′ : 4′-Pentamethoxyflavone is being prepared by a second method involving the reduction of 3 : 5 : 8 : 3′ : 4′-pentamethoxy-7-tosyloxyflavone.

EXPERIMENTAL

5-Hydroxy-3 : 3′ : 4′-trimethoxy-7-tosyloxyflavone (V)

5 : 7-Dihydroxy-3 : 3′ : 4′-trimethoxyflavone (14 g.) was dissolved in dry acetone (1,400 c.c.); *p*-toluenesulphonyl chloride (7·8 g., 1 mol.) and anhydrous potassium carbonate (45 g.) were added and the mixture was refluxed for 3 hours. Acetone was distilled off, the residue taken up in water and acidified. The precipitate was filtered, washed with water and dried; it crystallized from alcohol in yellow plates (15·1 g.), m.p. 157° (Found: C, 60·4; H, 4·5. $C_{25}H_{22}O_9S$ requires C, 60·2; H, 4·4%). The substance gives with aqueous caustic soda a sparingly soluble yellow sodium salt and with alcoholic ferric chloride a brown colour.

Reduction of 5-hydroxy-3 : 3′ :4′-trimethoxy-7-tosyloxyflavone

The tosyl ester (14 g.) was dissolved in alcohol (10 l.), Raney nickel prepared according to the method of Mozingo (140 g.) added, and the mixture agitated for one hour while a steady stream of hydrogen was led in. The mixture was then filtered and concentrated to a small bulk. The nickel residue was deactivated under hydrochloric acid, filtered, washed with water and the residue extracted with hot alcohol. The extract was added to the above concentrate, potassium hydroxide (7 g.) dissolved in a small amount of water added, and the solution refluxed for one hour. The alcohol was distilled off, the residue taken up in water and acidified. The precipitate (7·6 g.) was extracted with cold benzene and the benzene extract chromatographed on Florex. The yellow percolate on removal of the solvent gave a yellow substance which crystallized from methanol in pale yellow needles (4·2 g.), m.p. 153° (Found: C, 65·9; H, 5·1. $C_{18}H_{16}O_6$ requires C, 65·9; H, 4·9%). The substance, *5-hydroxy-3 : 3′ : 4′-trimethoxyflavone* (VI), gives a difficultly soluble yellow sodium salt with aqueous caustic soda and with alcoholic ferric chloride a green colour.

The residue undissolved by cold benzene (2·6 g.), after crystallization from alcohol, was identified as 5 : 7-dihydroxy-3 : 3′ : 4′-trimethoxyflavone by m.p. and mixed m.p.

5-Acetoxy-3 : 3′ : 4′-trimethoxyflavone

This was prepared by acetylation of (VI) (0·1 g.) by acetic anhydride (1 c.c.) and a drop of pyridine. It crystallized from methanol in long colourless silky needles, m.p. 157° (Found: C, 64·8; H, 5·2. $C_{20}H_{18}O_7$ requires C, 64·9; H, 4·9%).

5: 8-*Dihydroxy*-3: 3′: 4′-*trimethoxyflavone* (*VII*)

To a mechanically stirred solution of 5-hydroxy-3: 3′: 4′-trimethoxyflavone (VI) (3·0 g.) in pyridine (75 c.c.) and potassium hydroxide solution (5 g. in 125 c.c. water), a solution of potassium persulphate (5 g. in 250 c.c. water) was added slowly in the course of two hours. The brown solution was allowed to stand for 24 hours and acidified, when unchanged 5-hydroxy-3: 3′: 4′-trimethoxyflavone separated and was filtered off. The filtrate was extracted twice with ether to remove the last traces of the unreacted compound. The quantity of (VI) recovered was 0·6 g. After ether extraction, the clear brown aqueous layer was treated with sodium sulphite (10 g.) and conc. hydrochloric acid (100 c.c.) and heated on a boiling water-bath for 30 minutes. It was then cooled, and the yellow product which separated was filtered and washed with water. The filtrate on ether extraction gave more of the substance, but this was less pure. The product was first crystalized from ethyl acetate using a little Florex for removing the impurities, and then from methanol; the yellow needles (1·4 g.) had m.p. 212–13° (Found: C, 63·2; H, 4·9. $C_{18}H_{16}O_7$ requires C, 62·8; H, 4·7%). The substance dissolves in aqueous caustic soda to give a pinkish red solution; with alcoholic ferric chloride a brown colour is produced. On treatment with *p*-benzoquinone in alcoholic solution a dull red solid separates slowly (the gossypetone reaction).

The dihydroxy compound (VII) (0·1 g.) was acetylated with acetic anhydride (1·5 c.c.) and two drops of pyridine. The diacetate crystallized from alcohol in colourless needles, m.p. 190–91° (Found: C, 61·8; H, 4·8. $C_{22}H_{20}O_9$ requires C, 61·7; H, 4·7%).

3: 5: 8: 3′: 4′-*Pentahydroxyflavone* (*III*)

5: 8-Dihydroxy-3: 3′: 4′-trimethoxyflavone (0·4 g.) was dissolved in hot benzene (400 c.c.) and anhydrous aluminium bromide (2·4 g.), dissolved in benzene, was added slowly. A red precipitate of the complex was immediately formed. The mixture was refluxed for 3 hours and the benzene then distilled off. The residue was taken up in crushed ice and hydrochloric acid and, after the complete decomposition of the complex, the yellow product was filtered and washed. It was dissolved in acetone and carefully diluted with water when an oily material was thrown out. This impurity was removed, and the precipitate obtained by further dilution was crystallized thrice from aqueous acetone; the yellow needles (0·24 g.) had m.p. 270–71° (Found: C, 59.7; H, 3·6. $C_{15}H_{10}O_7$ requires C, 59·6; H, 3·3%). The mixed m.p. with ponderosin is 250–55°. The substance dissolves in 0·1 N aqueous caustic soda to a yellow-orange solution turning slightly pink. It

gives the same colour with aqueous potassium carbonate solution. The alcoholic ferric chloride colouration is green. The gossypetone reaction (with *p*-benzoquinone) yields a red solution.

3 : 5 : 8 : 3′ : 4′-*Pentacetoxyflavone*

The pentahydroxyflavone (0·1 g.) was acetylated with acetic anhydride (2 c.c.) and a few drops of pyridine. The acetyl derivative crystallized from alcohol in colourless rectangular plates, m.p. 236–37° (Found: C, 58·7; H, 4·0. $C_{25}H_{20}O_{12}$ requires C, 58·6; H, 3·9%). On admixture with the pentacetate prepared from ponderosin, the m.p. was depressed to 210–12°.

3 : 5 : 8 : 3′ : 4′-*Pentamethoxyflavone*

A mixture of (VII) (0·1 g.), acetone (10 c.c.), dimethyl sulphate (0·16 c.c.) and anhydrous potassium carbonate (1·0 g.) was refluxed for 12 hours. The mixture was cooled, filtered and the residue washed with a little acetone. The solvent was distilled off, the oily residue treated with 5% sodium carbonate solution (20 c.c.), and heated on a water-bath for one hour. The solution was cooled and the colourless needles which separated were filtered, washed and dried. Recrystallization from benzene-hexane gave colourless needles, m.p. 155° (Found: C, 64·3; H, 5·3. $C_{20}H_{20}O_7$ requires C, 64·5; H, 5·4%).

Methylation of ponderosin

A mixture of ponderosin (20 mg.), acetone (2 c.c.), anhydrous potassium carbonate (0·5 g.) and dimethyl sulphate (0·06 c.c.) was refluxed for 15 hours. The mixture was cooled, filtered and the residue washed with a little acetone. The product, obtained after the evaporation of acetone, crystallized from aqueous methanol in colourless needles, m.p. 173° (Found: C, 63.9; H, 5.8. $C_{20}H_{20}O_7$ requires C, 64·5; H, 5·4%).

SUMMARY

By Raney nickel hydrogenolysis of the 7-tosyl ester (V), 5 : 7-dihydroxy-3 : 3′ : 4′-trimethoxyflavone (IV) has been converted into 5-hydroxy-3 : 3′ : 4′-trimethoxyflavone (VI). Persulphate oxidation of (VI) gave 5 : 8-dihydroxy-3 : 3′ : 4′-trimethoxyflavone (VII), which was demethylated to 3 : 5 : 8 : 3′ : 4′-pentahydroxyflavone (III) by means of aluminium bromide in benzene. This pentahydroxyflavone was different in its properties from ponderosin, the yellow colouring matter of *Ponderosa* pine bark.

ACKNOWLEDGMENT

We are greatly indebted to Dr. E. F. Kurth for a sample of ponderosin. We are grateful to the Ministry of Education, Government of India, for the

award of a Fellowship to one of us. Our thanks are due to Dr. T. S. Gore for the microanalyses recorded in the paper, and to the Floridin Co., Inc., Warren, Pa., U.S.A., for a gift of Florex.

References

1. Kurth and Hubbard .. *Ind. Eng. Chem.*, 1951, **43**, 896.
2. Wilson .. *J. Am. Chem. Soc.*, 1939, **61**, 2303.
3. Row and Seshadri .. *Proc. Ind. Acad. Sci.*, 1945, **21A**, 130, 155.
4. Ramanathan and Venkataraman .. *Curr. Sci.*, 1952, **21**, 283.
5. ———— .. *Proc. Ind. Acad. Sci.*, 1953, **38A**, 40.
6. Kenner and Murray .. *J. Chem. Soc.*, 1949, S 178.
7. Allan and Robinson .. *Ibid.*, 1926, 2334.
8. Rao and Seshadri .. *Proc. Ind. Acad. Sci.*, 1947, **25A**, 417, *et sequa*.
9. Shah, Mehta and Wheeler .. *J. Chem. Soc.*, 1938, 1555.
10. Briggs and Locker .. *Ibid.*, 1949, 2157; 1951, 3131.
11. Rao, Seshadri and Viswanadham *Proc. Ind. Acad. Sci.*, 1949, **29A**, 72.
12. Mozingo, Wolf, Harris and Folkers *J. Am. Chem. Soc.*, 1943, **65**, 1013.

A STURDY THERMOELECTRIC PSYCHROMETER FOR MICROCLIMATIC MEASUREMENTS

By K. Raschke

Received October 10, 1953
(Communicated by Dr. L. A. Ramdas)

To the microclimatologist who wishes to record the fine structure of the variations with time or space the measurement of humidity presents certain instrumental problems as the instruments generally used in meteorology prove to be unsuitable for this purpose. The conventional hair-hygrometer which has too large dimensions can only be used for the measurement of the mean humidity of air layers. The psychrometer which is the other instrument most commonly used in meteorology for the measurement of humidity does not function satisfactorily without aspiration and disturbs the microclimatic structure of a small space completely. Moreover, both instruments mentioned above, have too long time constants which do not permit their use for observations of rapid changes in humidity.

In 1932, Wald[1] and in 1936 Koch[2] developed psychrometers which employed wet elements with a diameter of only 1 mm. which did not require any ventilation. These two workers as well as Rossi (1933)[3] utilised small thermocouples for the translation of temperature differences into emfs thus permitting distant reading and recording. But non-ventilated thermocouple psychrometers have not come into general use by microclimatologists on account of their not yet having reached technical perfection.

Only recently a thermocouple psychrometer developed by Diem and reported to be working satisfactorily is mentioned in a paper of Trappenberg[4] but no technical details have been given. The present writer has designed a non-ventilated thermo-electric psychrometer for microclimatic measurements. When the instrument was completed a publication by Unger[5] on thermocouple psychrometers appeared. The instrument to be described in this paper differs from Unger's in certain features especially in the construction of the "wet" thermocouple. Furthermore, the radiation error being the only error of the instrument larger than the accuracy of the usual recording devices, it can be compensated utilising a new method. The instrument was designed for use even in heavy rains and gusts.

The psychrometer to be described in this paper employs a "wet" junction having a diameter of less than 1 mm. similar to the "wet" junctions of

the instruments of Wald and Koch. In case the " wet " junction has the dimensions mentioned above, the psychrometric difference has already reached its maximum in still air and ventilation has no further influence on it. Hence the temperature of the " wet " junction depends only on the saturation deficit of the surrounding air.

The " wet " element is kept moist by means of a cotton thread twisted round the thermocouple and which passes into a small feed tank containing distilled water. Since the water evaporating from the exposed part of the wick influences the humidity of a small space the exposed evaporating surface of the wick should be kept at its minimum. To make a rough estimate of the minimum dimensions of the evaporating part, we assume a thread consisting only of water (the heat conductivity of cellulose is only about one-third of that of water) connected to a water reservoir, the temperature of which is assumed to be at air temperature. Each slab of the thread gains heat by conduction from the water reservoir and loses heat partly by evaporation and by conduction to the next slab. Another quantity of heat is received from the surroundings by convection and radiation and is a function of the temperature difference between the air and the slab. The temperature distribution along a wet thread may be represented by

$$\frac{\partial\theta}{\partial t} = \frac{K\partial^2\theta}{c\rho\partial x^2} - \frac{Lp}{c\rho\omega} + \frac{Hp\theta}{c\rho\omega} \qquad (1)$$

where

L = heat lost by evaporation per unit area per unit time (a function of the saturation deficit of the air),

H = heat transfer coefficient of the thread,

K = heat conductivity of the thread,

c = specific heat of the thread,

ρ = density of the thread,

p = perimeter of the thread,

ω = cross-section of the thread.

For the steady temperature state we get

$$O = \frac{d^2\theta}{dx^2} - \frac{Lp}{K\omega} + \frac{Hp\theta}{K\omega} . \qquad (2)$$

Since there is no flow of heat from the end of the thread, our solution is given by

$$\theta_e = \theta_w \frac{\cosh \mu (l - x)}{\cosh \mu l} \qquad (3)$$

on putting

$\mu = \sqrt{\frac{Hp}{K\omega}}$

l = length of the evaporating part of the thread,

θ_w = psychrometric difference,

θ_e = temperature error.

Hence the temperature error at the end of the thread is

$$\theta_e = \frac{\theta_w}{\cosh \mu l}$$

and the minimum length l_{min} of the wet thread for the maximum permissible error $\theta_{e_{max}}$ is

$$l_{min} = \frac{\cosh^{-1} \theta_w/\theta_{e_{max}}}{\mu} . \qquad (4)$$

If we use

$K = 0{\cdot}0014$ cal °C.$^{-1}$ cm.$^{-1}$ sec^{-1},

$H = 0{\cdot}0007$ cal cm.$^{-2}$ sec^{-1},

$p = 0{\cdot}157$ cm. (diameter of the thread $= 0{\cdot}05$ cm.),

$\omega = 0{\cdot}00196$ cm.^{2},

and if we permit a maximum error of 0·1° C. at a psychrometric difference of 20° C. we obtain

$$l_{min} = \frac{\cosh^{-1} 200}{6{\cdot}3} = \frac{6}{6{\cdot}3} = 0{\cdot}95 \approx 1 \text{ cm.}$$

This value is in good agreement with the experimental results obtained with " wet " thermocouples of different lengths at low humidities.

The question for the minimum length of a wire placed in the centre of a wet thread of uniform temperature and adopting the temperature of the wick now remains to be considered. The wire is assumed to be made of constantan (conductivity 0·05) with a diameter of 0·01 cm., and to be coated with an insulating layer (conductivity 0·0005) of 0·005 cm. thickness. For 1° C. temperature difference between inner and outer surface of the insulating layer 0·1 cal. are conducted through an area of 1 cm.^{2} coating per second. This is the heat transfer coefficient of the wire.

Again we use the equation of conduction

$$\frac{\partial \theta}{\partial t} = \frac{K \partial^2 \theta}{c\rho \partial x^2} - \frac{Hp\theta}{c\rho\omega} \qquad (5)$$

where the thread is supposed to be at zero temperature*. For a finite wire we obtain the special solution analogous to (3)

$$\theta_e' = \frac{\theta_w' \cosh \mu' (l' - x)}{\cosh \mu' l'}$$

where θ'_w is used for the temperature of the wire before entering the wet thread. The equation for the minimum length is analogous to (4)

$$l'_{\min} = \frac{\cosh^{-1} \theta_w'/\theta_e'}{\mu'}$$

Using 20° C. for θ'_w and 0·01° C. for θ'_e we get

$$l'_{\min} = \frac{\cosh^{-1} 2000}{28} = \frac{8 \cdot 3}{28} = 0 \cdot 3 \text{ cm.}$$

The minimum length for a copper wire of the same dimensions but with a heat conductivity of 0·9 is

$$l'_{\min} = \frac{\cosh^{-1} 2000}{6 \cdot 7} = \frac{8 \cdot 3}{6 \cdot 7} = 1 \cdot 2 \text{ cm.}$$

Two types of "wet" thermocouples can be used. In the first pattern the thermocouple is strung between two points the junction being somewhere between the points of suspension (Fig. 1 *a*). A wet wick covers the junction as well as a part of both the copper and the constantan wires. The wick is

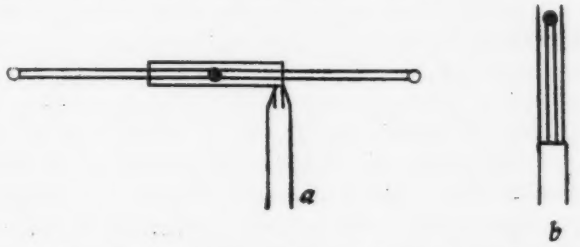

FIG. 1. "Wet" thermocouple, *a*: "L" type, *b*: needle type.

fed on the constantan side. If we assume the dimensions given in the examples calculated above, the wick has attained the correct "wet bulb" temperature after 1 cm. evaporating length. The constantan wire in its centre will obviously have adopted the same temperature at the junction. According to our estimations, the wick should cover at least 1·2 cm. of the copper arm of

* The heating of the thread by the wire has been neglected in this calculation as well as in the following estimations.

the element. Therefore the minimum total evaporating length of this type of " wet " thermocouple amounts to 2·2 cm.

The second type of " wet " thermocouple has the shape of a needle with the junction at its tip (Fig. 1 *b*). Since in this pattern the copper and constantan wire form a self-supporting thermocouple, the mechanical strain is much smaller than in the first pattern which enables a much thinner copper wire to be used. The use of the thin wire requires a shorter length of the evaporating wick for the copper wire to attain the correct " wet bulb " temperature, *e.g.*, 0·9 cm. for a copper wire of 0·005 cm. diameter if there is no temperature gradient along the wick. Since the temperature of the wick changes with increasing distance from the feed tank according to (1), equation (4) is to be changed into

$$\frac{\partial\theta}{\partial t} = \frac{K\partial^2\theta}{c\rho\partial x^2} - \frac{Hp}{c\rho\omega}\left(\theta - \frac{\theta_w \cosh\mu(l-x)}{\cosh\mu l}\right)$$

from which we obtain for the temperature error at the end of the needle

$$\theta_e = \frac{\theta_w}{(l-\mu^2/\mu'^2)}\left(\frac{1}{\cosh\mu l} - \frac{\mu^2/\mu'^2}{\cosh\mu' l}\right).$$

For a self-supporting " wet " thermocouple of 1 cm. length and 0·05 cm. diameter made of a 0·01 cm. constantan wire and 0·005 cm. copper wire the error is calculated to be 0·13° C. at a psychrometric difference of 20° C. Actually, the error will be smaller as the coating of the thermocouple is usually thinner than 0·005 cm. as assumed above, and it was experimentally determined that a needle-shaped " wet " thermocouple of the dimensions already mentioned developed an emf corresponding with the correct " wet bulb " temperature even at very low humidities. Therefore, we arrive at the conclusion that the needle pattern is preferable to the ' L ' pattern as it needs for the same maximum permissible error only half the evaporating surface of the ' L ' pattern. This means that a needle pattern " wet " thermocouple using an equal evaporating surface has a much smaller error than an ' L ' type thermocouple.

For the construction of the " wet " needles, enamelled copper wires with a diameter of 0·005 cm. (47 S.W.G.) and constantan wires with a diameter of 0·01 cm. (42 S.W.G.) have been used. The tip of the copper wire is soldered to the constantan wire at a distance of 0·5 cm. from its end (Fig. 2). Both wires are twisted together, dipped into a Bakelite solution and baked for several hours at 120° C. Special precaution should be taken that no free metallic surface is left exposed, otherwise the wet wick is liable to get spoiled by the corrosion products.

The thermocouple is passed through a capillary tube together with a white cotton thread. Then the thread is split and its fibres are twisted round the thermocouple (Fig. 2) and fixed to the tip of the constantan wire by means of a tiny drop of a cellulose cement. Under no circumstances the cement should be allowed to penetrate through the wick upto the junction.

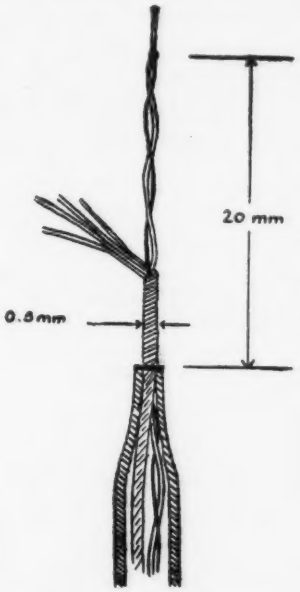

FIG. 2. Construction of the "Wet" needle, black: copper, white: constantan.

A length of 2 cm. has been chosen as a standard size of the " wet " needles and the diameter of this needle soaked with water is about 0·05 cm. It is advisable to have at hand a few extra " wet " elements inserted in suitable corks as replacement for dirty ones, whenever required.

The " dry " thermocouple of the psychrometer has been made of 0·01 cm. diameter (42 S.W.G.) copper and constantan wires joined together over a small spirit lamp using silver solder and borax as a flux. Such junctions are only slightly thicker than the diameter of the wire and are more resistant to mechanical strains than the copper wire of the thermocouple. The length of the " dry " element is determined by the maximum permissible error caused by heat conduction between junction and the support of the thermocouple. Using the copper constantan combination mentioned and taking 0·1° C. as the maximum error permitted at a temperature difference

of 5° C. between the support and the air, the constantan wire should be made 2 cm. long and the copper wire 8 cm.

A fork has been found to be the most suitable design of the support. Its prongs are made of Perspex, a transparent plastic, which absorbs no radiation in the visible part of the spectrum and is a poor heat conductor. This eliminates the errors caused by heat conduction during periods of strong insulation.

The end of the prong carrying the constantan leads is shielded against radiation by means of a small polished piece of aluminium (S in Fig. 3) protecting the junction of constantan (thin)—constantan (thick) from being

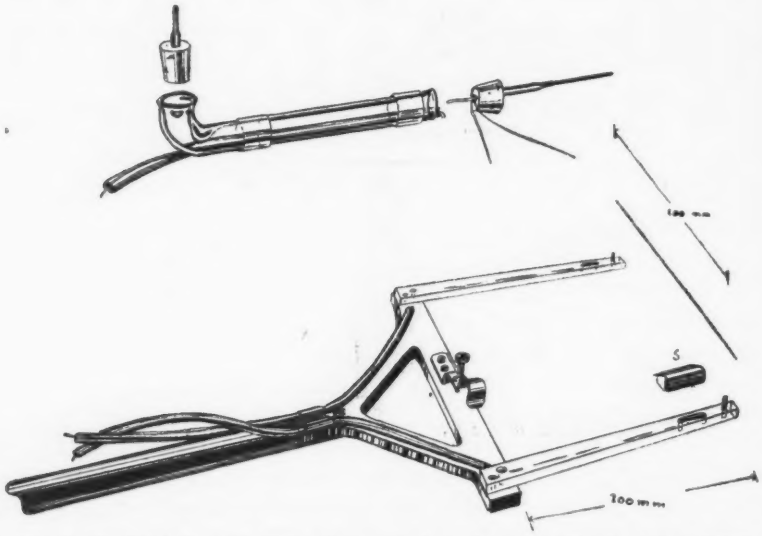

FIG. 3. Exploded diagram of the thermocouple psychrometer (*S*=aluminium shield)

heated above air temperature and thus preventing the introduction of an additional emf into the measuring element†). For the same reason the thick constantan wire is connected directly to the reference junction without an intervening plug.

The common reference junction of the instrument is coated with several layers of a chlorinated rubber paint securing a good thermal contact with the bath of reference temperature and at the same time complete insulation

† It has been observed that a small emf is always produced even in a constantan-constantan junction if a temperature difference is established (in this case it is of the order of 0·9 μV/°C).

against the other junctions kept in the same flask. Each layer of paint should be allowed to dry properly (for 24 hours) before applying the next layer.

The " wet " thermocouple forms together with the water tank the " wet unit " which easily can be replaced in the thermocouple psychrometer whenever required. The fixing rod permits the instrument to be mounted in any required position.

The measurement of the emfs developed is usually made with galvanometers. Since galvanometers are measuring currents the resistance of the " dry " element should be rendered equal to that of the " wet " one so that the same calibration of the galvanometer scale can be used for " dry " as well as for " wet " temperatures. The adjustment of the resistance can be made by taking a suitable length of the thin constantan wire of the " dry " thermocouple, the additional wire being wound round the prong of the support before soldering it to the thicker leading wire.

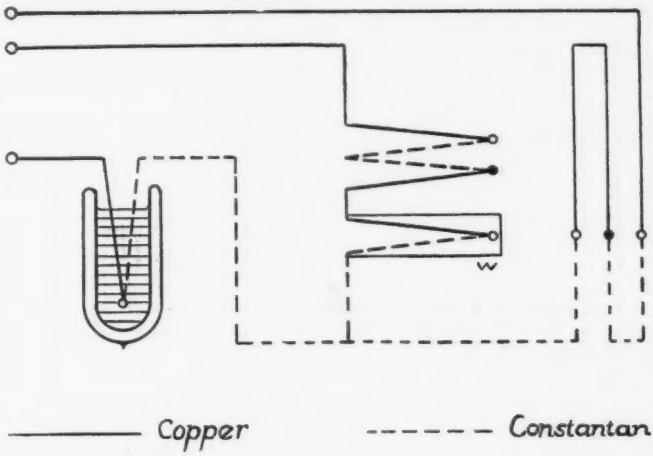

FIG. 4. Circuit of the thermocouple psychrometer compensated for the radiation error

The radiation error of the instrument can be compensated by introducing into the circuit consisting of the measuring junction, reference junction, and the measuring instrument, a second thermocouple in opposition with both its junctions exposed to the radiation. The junctions of the compensating element are made such that they differ in their radiation errors and that the difference in their radiation errors equals the radiation error[7] of the measuring junction. Details of this method will be given elsewhere, and the circuit is shown in Fig. 4. Instead of one " dry " measuring element

of the uncompensated instrument there are three elements strung parallel from prong to prong at a distance of 0·5 cm. from each other. Since the absorptivity of the elements is 0·5 the central element has been blackened by means of camphor soot suspended in a very dilute solution of a cellulose lacquer which resulted in an absorptivity of almost 1·0. The same method has been utilised for the elimination of the radiation error of the " wet " thermocouple. Both arms of the compensating element are constructed as needles like the " wet " measuring element but coated with a cellulose lacquer. The central junction of this set has been made grey such that the radiation error of the " wet " junction was always balanced. Even at very large psychrometric differences (22° C.) the error of the " wet " junction described above, caused by the non-linearity of the emf as a function of the temperature is less than 0·05° C.

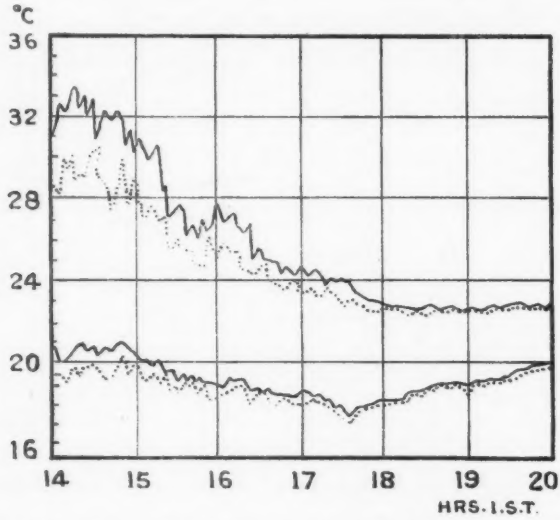

FIG. 5. "Dry" temperatures (upper two curves) and " wet " temperatures (lower two curves) at 10 cm. (straight lines) and 60 cm. (broken lines) above bare soil

Unger[5] has employed another method for the elimination of the radiation error of the " wet " junction of his instrument. He exposed the reference junction of the " wet " thermocouple to the air too. If the radiation error of the reference junction is equal to the radiation error of the " wet " junction the psychrometric difference between the junctions is not affected by the radiation (Robitzsch[6]). If this method is utilised the scale of the galvanometer should be calibrated in mV and not in °C.

A number of the psychrometers described in this paper has been made in the Meteorological Office at Poona and will be used for microclimatological and micro-meteorological studies close to the ground, close to large leaves and inside crops. A typical family of curves drawn after a record obtained by means of a Cambridge Thread Recorder without amplification of the emfs is shown in Fig. 5. In this record the accuracy of the reading is 0·2° C.

This work was carried out while the author held a scholarship granted by the Government of India under the Indo-German Industrial Co-operation Scheme. He is greatly indebted to Dr. L. A. Ramdas, Deputy Director-General of Observatories, for his keen interest and facilities given and wishes to thank Mr. S. P. Venkiteshwaran and the staff of the workshop of the Meteorological Office, Poona, for their support.

BIBLIOGRAPHY

1. Wald, H. .. *Z. f. d. ges Kälteindustrie*, 1932, **39**, H. 6.
2. Koch, W. .. *Gesundheits-Ingenieur*, 1936, **59**, 504–05.
3. Rossi, V. .. *Soc. Scient Fennica*; *Com. Phys. Math.*, 1933, **6**, 25, 1–22.
4. Trappenberg, R. .. *Arch. Met. Geoph. u. Biokl.*, 1952, **B4**, 65–84.
5. Unger, K. .. *Angew. Met.*, 1953, **1**, 279–83.
6. Robitzsch, M. .. In, Kleinschmidt, *Handbuch der meteorologischen Instrumente*, Berlin, 1935, 211.
7. Raschke, K. .. *Arch. Met. Geoph. u. Biokl.*, 1954, **A5**.

(1, 2 quoted after R. Geiger, "Das Klima der bodennahen Luftschicht," Braunschweig, 1950).

196-54 Printed at The Bangalore Press, Bangalore City, by C. Vasudeva Rao, Superintendent
and Published by The Indian Academy of Sciences, Bangalore

NOTICE TO AUTHORS

Scientific papers intended for publication in the *Proceedings of the Indian Academy of Sciences* can be accepted only when they are communicated by a Fellow of the Academy whose duty shall be to satisfy himself that such communications are fit to be read at the Meeting of the Academy and published in its *Proceedings*.

Papers should not ordinarily exceed fifty pages of foolscap. MSS. should be either typewritten or written in legible hand on one side of the paper. All papers should be carefully revised by the authors and should be absolutely in final form for printing. Position for text-figures should be indicated. Each paper shall conclude with a critical summary not exceeding 350 words.

Drawings, diagrams or other illustrations should be made on larger scale (preferably) twice the size than the ones in which they are intended to appear. They should be done in Indian ink on bristol board with lettering in pencil. Scale of magnification of camera lucida tracings should be indicated by the side of drawings. In certain special cases arrangements will also be made for monochrome lithographic and other colour plates. Reduction of illustrations desired should be indicated in pencil. Appropriate legends should accompany all drawings. Names of authors are to be marked in pencil on the left-hand corner of drawing sheets. Photomicrographs should be securely mounted with colourless paste.

All tables, quotations and footnotes which will be set hereafter (beginning from Vol. I, No. 2) in types smaller than the text, should be typewritten on separate sheets and placed with the text in proper sequence. Footnotes should be numbered in Arabic numerals.

References to literature in the text should be given, whenever possible, in chronological order, only the names of authors and years of publication, in brackets, being given. They should be cited in full after the summary, the authors' names following in alphabetical order. Thus,

Name or Names of author; Name of Journal (abbreviation) with a single underline; Year of publication; Number of Volume with a double underline, and lastly page. The following would be a useful illustration:—

Bergmann and Stather . . . . . Z. Physiol. Chem., 1926, 152, 189.

Two copies of slip-proof and wherever possible, a page proof for final revision will be sent to authors. All corrections are best made on the slip-proof which should be transmitted to the Office of the Academy. All proof corrections involve heavy expenses which would be negligible if the papers are carefully revised by the authors before submission.

Authors will be supplied with reprints of their papers at cost price, if intimation is given at the time of returning the slip-proof.

Blocks appearing in the *Proceedings* will be available for purchase by their respective authors. Orders for the same should be sent along with the corrected proofs and in any case not later than one month after the date of publication of the paper. The price charged would be 25% of the actual cost of the blocks *plus* freight and despatching charges. If the blocks are reproduced in other journals or publications, due acknowledgment should be made in them to the *Proceedings*.

The original drawings and plates of blocks appearing in the *Proceedings* will be returned to such of the authors as may require them provided the cost of despatching such originals is borne by them.

CONTENTS

PAGE

X-Ray Anti-Reflections in Crystals. Part II. Calculation of the Integrated Reflection and Integrated Anti-Reflection for an Internal Reflection . . . . . G. N. Ramachandran 65

The Infra-Red Absorption Spectrum of Barytes . . . . A. K. Ramdas 81

Synthetical Experiments in the Chromone Group. Part XXX. A Synthesis of 3 : 5 : 8 : 3′ : 4′-Pentahydroxyflavone and Its Non-Identity with Ponderosin . . . . . V. Ramanathan and K. Venkataraman 90

A Sturdy Thermoelectric Psychrometer for Microclimatic Measurements . . . . . K. Raschke 98